ABANT IZZET BAYSAL UNIVERSITY

THE GRADUATE SCHOOL OF NATURAL AND APPLIED SCIENCES

DEPARTMENT OF CHEMISTRY

SYNTHESIS OF HEXAGONAL BORON NITRIDE IN THE PRESENCE OF METAL OXIDES

MASTER OF SCIENCE

ERKAM GÜLLÜOĞLU

BOLU, JULY 2015

APPROVAL OF THE THESIS

SYNTHESIS OF HEXAGONAL BORON NITRIDE IN THE PRESENCE OF METAL OXIDES submitted by **Erkam GÜLLÜOĞLU** in partial fulfillment of the requirements for the degree of Master of Science in **Department of Chemistry, Abant Izzet Baysal University** by,

Examining Committee Members	**Signature**
Supervisor Prof, Çetin Bozkurt, Abant Izzet Baysal University	.....
Member Assist. Prof. Erhan Budak, Abant Izzet Baysal University	.....
Member Assist. Prof. Muhammed Öz, Gerede Vocational School	.....

July 24, 2015

Prof. Dr. Duran KARAKAS .....

Director, **Graduate School of Natural and Applied Sciences**

To my family

DECLARATION

I hereby declare that all information in this document has been obtained and presented in accordance with academic rules and ethical conduct. I also declare that, as required by these rules and conduct, I have fully cited and referenced all material and results that are not original to this work.

Erkam GÜLLÜOĞLU

ABSTRACT

SYNTHESIS OF HEXAGONAL BORON NITRIDE IN THE PRESENCE OF METAL OXIDES
MSC THESIS
ERKAM GÜLLÜOĞLU
ABANT IZZET BAYSAL UNIVERSITY GRADUATE SCHOOL OF NATURAL AND APPLIED SCIENCES
DEPARTMENT OF CHEMISTRY
(SUPERVISOR: PROF. DR. ÇETİN BOZKURT)

BOLU, JULY 2015

Boron nitride is an engrossing material in the area of materials science. Being isoelectronic of both boron and nitrogen to carbon brings the special bonding behaviours which leads BN able to occur in several different structures. Variety in structures bring forth the different chemical and physical properties proper to the use of different industrial areas.

In this study, hexagonal boron nitride was synthesized by the modified O'Connor method in presence of various metal oxides. The analysis for determining the structural properties of the synthesized materials were done by X-Ray Diffraction, (XRD), Fourier Transform Infrared Spectroscopy, (FTIR), and Scanning Electron Microscopy, (SEM).

The verification of the hexagonal boron nitride, (hBN), formation is achieved by the main peaks in results of FTIR, XRD respectively. The lattice parameters of samples were calculated and exposed to be very close to the original hBN. The grain size calculations and SEM analysis confirmed the nano-scale of the synthesized products.

KEYWORDS: Hexagonal Boron Nitride, O'Connor Method, Metal Oxide, Synthesis

ÖZET

METAL OKSİT VARLIĞINDA HEKZAGONAL BOR NİTRÜR SENTEZİ
YÜKSEK LİSANS TEZİ
ERKAM GÜLLÜOĞLU
ABANT İZZET BAYSAL ÜNİVERSİTESİ FEN BİLİMLERİ ENSTİTÜSÜ
KİMYA ANABİLİM DALI
(TEZ DANIŞMANI: PROF. DR. ÇETİN BOZKURT)

BOLU, TEMMUZ - 2015

Bor nitrür, malzeme bilimleri alanında ilgi çekici bir konudur. Bor ile azotun karbona izoelektronik olmasının getirdiği özel bağlama davranışları bor nitrürün bazı farklı yapılarda bulunabilmesini sağlar. Yapılardaki farklılık değişik endüstriyel alanlardaki kullanıma uygun farklı kimyasal ve fiziksel özelliği getirir.

Bu çalısmada, hekzagonal bor nitrür modifiye O'Connor metodu ile çeşitli metal oksitlerinin varlığında sentezlenmistir. Sentezlenen maddelerin yapısal özelliklerini saptama analizleri X-Isını Kırınım Ölçeri (XRD), Fourier Dönüsüm Kızılötesi Spektroskopisi (FTIR) ve Taramalı Elektron Mikroskobu (SEM) kullanılarak yapılmıştır.

Hekzagonal bor nitrür oluşumunun doğrulanması sırasıyla FTIR ve XRD sonuçlarındaki ana piklerle elde edilmiştir. Numunelerin örgü parametreleri hesaplanmış ve orjinal hexagonal bor nitrüre çok yakın bulunmuştur. Tanecik büyüklüğü hesaplamaları ve SEM analizleri sentezlenen maddelerin nano ölçekte olduğunu doğrulamıştır.

ANAHTAR KELİMELER: Hekzagonal Bor Nitrür, O'Connor Metot, Metal Oksit, Sentez

TABLE OF CONTENTS

Page

LIST OF FIGURES

Page

LIST OF TABLES

Page

LIST OF ABBREVIATIONS AND SYMBOLS

2θ	**:** Bragg angle degree
BN	**:** Boron Nitride
cBN	**:** Cubic Boron Nitride
EDX	**:** Energy Dispersive X-Ray Spectroscopy
hBN	**:** Hexagonal Boron Nitride
ICDD	**:** The International Centre for Diffraction Data
rBN	**:** Rhombohedral Boron Nitride
SEM	**:** Scanning Electron Microscopy
tBN	**:** Turbostratic Boron Nitride
wBN	**:** Wurtzitic Boron Nitride
XRD	**:** X-Ray Diffractometer

ACKNOWLEDGEMENTS

I wish to express my deepest gratitude to my supervisor Prof. Dr. Çetin BOZKURT for his guidance, advice, criticism, encouragements and insight throughout the research.

I would also like to thank Assist. Prof. Dr. Erhan BUDAK for his suggestions and comments. His friendship as an elder brother and guidance as an advisor helped me in all the time of research and writing of this thesis. I could not have imagined having a better consultant in this M.S. study.

My sincere thanks also goes to Assist. Prof. Dr. Muhammed ÖZ for his suggestions and instructions during the experimental procedures. His friendship and instructions helped me to get better result on experiments.

I would like to express my gratitude to Prof. Dr. Ahmet VARİLCİ for his laboratory support and also Nevin SOYLU for her support and help in analysis of samples.

Besides, I am also grateful to Muhammet Turhan, Ali Osman Çetinkaya, Nuşin Sunar, Canan Sapmaz and Ercan Ünlü for their sincere friendship and motivation during this study.

Last but not the least; I would like to thank to my family for their endless support, love, patience and prayers for me that made the accomplishment of this work.

Finally, I would like to express my deepest gratitude to my beautiful wife Leyla Güllüoğlu and my unborn daughter Zehra Hicaz Güllüoğlu, who were the very main supports and my source of tranquility with their existence, by means of them that I am able to complete this study.

1. INTRODUCTION

Boron compounds may have been known for about 6000 years, starting with the Babylonians. The Egyptians, Chinese, Tibetans and Arabians are reported to have used such materials. The Arabs used the expression «buraq» for a number of minerals including the now familiar borax. Today Turkey has the largest boron ore deposits in the World. Also, boron and its compounds were declared by USA and NATO as strategically important material in 1961 (Chamber of Mining Engineers of Turkey, 2008).

Boron nitride (BN) – in all its various structures – is a synthetic product and not found in nature. The first synthesis for hexagonal boron nitride (hBN) was described in 1842 by Balmain (Balmain, 1842), but hBN became a commercial material after 100 years. Due to its excellent properties hBN is useful for industrial applications:

i. For the lubricity, hBN does not need any extra medium between the layers, so hBN lubricants can be used even in vacuum, e.g. for space applications.
ii. Due to its excellent dielectric and insulating properties, hBN is used in electronics e.g. as a substrate for semiconductors, microwave-transparent windows, structural material for seals, electrodes and catalyst carriers in fuel cells and batteries.
iii. hBN is quite chemically inert and is not wetted by many melted materials (e.g. aluminum, copper, zinc, iron and steels, germanium, silicon, boron, cryolite, glass and halide salts).
iv. Chemically and physically stabilization causes hBN to have many application areas in industry.

The most suitable process of preparing boron nitride ceramics is hot pressing through the strong covalent bond character of boron and nitrogen within macromolecular layers. The well-crystallized phase was occurred at high temperature (1650 C° and above), whereas low temperature forms prepared at about 1000°C causes irregular structure (turbostratic boron nitride, tBN) (Yucel, 2005).

In 1993, addition of B_2O_3 was found to be effective on the crystallization of amorphous BN and increased crystallinity of BN at high temperature (1350 – 1450°C) by Choi et al. The amorphous BN with B_2O_3 were crystallized and transformed to cBN with catalyst (Choi et al, 1993). In 1996, chemical reactions of hBN synthesis and their mechanisms are discussed by Hubacek and Ueki. They were suggested a ternary B-N-O diagram for virtual compositions of hBN ceramic and preceding materials (Hubacek and Ueki, 1996).

Later, hBN was hot pressed in copper environment. It was sighted that thickening and aligning of the grains in contrast to the system without copper when subjected of metal. It was also found that the copper metal cause boron nitride layers in hexagonal form to lined up with interlaying spacing as short as 0.3328 nm (Hubacek et al, 1997).

In another study, hBN were synthesized by the modified O'Connor method in the presence of various metal nitrides and the crystallization degree and grain growth of hBN can be improved by intercalation with various transition metals at a relatively lower temperature (1050°C) by Budak and Bozkurt. They suggested that interlayer spacing was affected due to the electronic interaction between hBN and valance orbital of metal and the reduction reaction between the metal and hBN overcomes the internal stress (Budak and Bozkurt, 2004).

1.1 Theory of boron nitride

1.1.1 Structure of boron nitride

Boron nitride (BN) is a modern man made compound that perfectly parallels the crystalline structure and properties of naturally occurring elementary carbon. This, causing the boron nitride as a material that is center of interest in both material science and technology.

Since both boron and nitrogen are isoelectronic to the carbon, resulting the various structural forms which can be classified in three main groups: Turbostratic boron nitride, tBN, cubic boron nitride, cBN, hexagonal boron nitride, hBN.

tBN is similar to hBN but the order in the direction of axis c is disturbed. Actually each hexagonal layer may be twisted in a random way against its neighbor layers. As a result the tridimensional order is limited and the spacing between the hexagonal layers increased by 3-4% in comparison with a perfectly ordered structure (Petrescu and Balint, 2007). The disordered structure, resulting from weak attractive forces between layers, consists in irregularities of the layers arranging within the c crystallographic axis (Hubacek et al, 1996).

cBN have tridimensional lattices in which each atom is in an sp^3 hybridization state and establishes four strong covalent σ bonds with its nearest neighbors that make up tetrahedron around it. No more π electrons are available to give rise to a weak bond and this explains the high hardness and insulating character of the high density BN polymorph (Petrescu and Balint, 2007). The cubic form is approximately as hard as diamond and, more important, has a higher oxidation resistance.

hBN, as known as white graphite (Figure 1.1.), crystallizes similar to graphite in a hexagonal sheet layered structure. Furthermore, hBN shows different characteristic from the cBN with sp^2 hybridization. Due to the higher electronegativity of nitrogen and π-electron is located at the nitrogen and therefore hBN is an electrical insulator and its color is white. The covalent bonds (σ-bonding) between atoms in the ring are very strong. The strong bonds between B and N atoms within the hexagonal layers has however an ionic component due to the presence of two atomic species with different electronegativity. Besides, the bond between hexagonal layers, between the atomic planes (π-bonding), is extremely weak, van der Waals bonds. This explains its far higher length (3.3306 Å in comparison with the short length 1.4457 Å) of the strong covalent bond within the hexagonal layers. As a result of the extremely weak interlayer bonds, hBN has a higher lubricity at both low and high temperatures (up to 900°C, even in an oxidizing atmosphere or in vacuum).

This property brings that the lubricity of h-BN does not require water or gas molecule trapped between the layers which is an advantage of hBN over graphite.

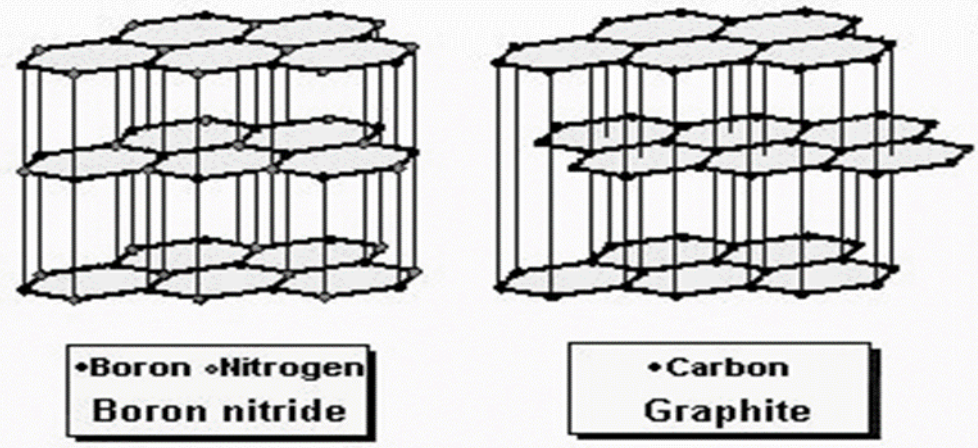

Figure 1.1. Structure of hexagonal boron nitride and graphite.

1.1.2 Synthesis of boron nitride

The first synthesis for hBN was described in 1842 by Balmain by reaction of molten boric acid with potassium cyanide (Balmain, 1842). It took until the 1940s before it gained limited economic significance. Process improvements have led to more economical and higher quality BN qualities (Lipp et al 1989). Since that time, there have been many methods developed for synthesis of hBN, but above all principally two methods are used on the industrial scale.

1.1.3 Boric Acid with Carrier Substances

Boric acid with ammonia reacts in the presence of carrier substances ($Ca_3(PO_4)_2$, $CaCO_3$, CaO, BN, Zn-borate). The carrier substances prevent the formation of a homogeneous melt of boric acid, which is not suitable because of its minimal surface: At reaction temperatures exceeding 700°C a thin film of molten boric acid covers each carrier substance particle. Because of the large surface a full reaction of the boric compound with ammonia is possible. After the reaction the carrier is leached with HCl and the remaining hBN is washed with water. A second

reaction at temperatures exceeding 1500°C with ammonia follows, resulting in hBN powders with 97% purity. The hBN crystallites are thin hexagonal platelets with a thickness of about 0.1-0.5 µm and a diameter up to 5 µm.

1.1.4 Boric Acid with Organic Nitrogen Compounds

The second important way to produce hBN is the reaction of boric acid or alkali borates with organic nitrogen compounds (melamin, urea, dicyanamide, guanidine) in nitrogen atmosphere. These reactions are carried out at temperatures between 1000°C and 2100°C in N_2 atmosphere. Before final thermal treatment, the product can be washed with methanol or diluted acids in order to remove all non-reacted products. For removing oxygen impurities a thermal treatment at 1500°C in inert N_2 or Ar atmosphere is used. BN with tBN is obtained which is characterized by partial or complete absence of three-dimensional order in the stacking of its atomic planes (Haubner et al, 2002).

There have been many methods developed on synthesis of hBN. But for a comparison, a common chart described as following Figure 1.2.

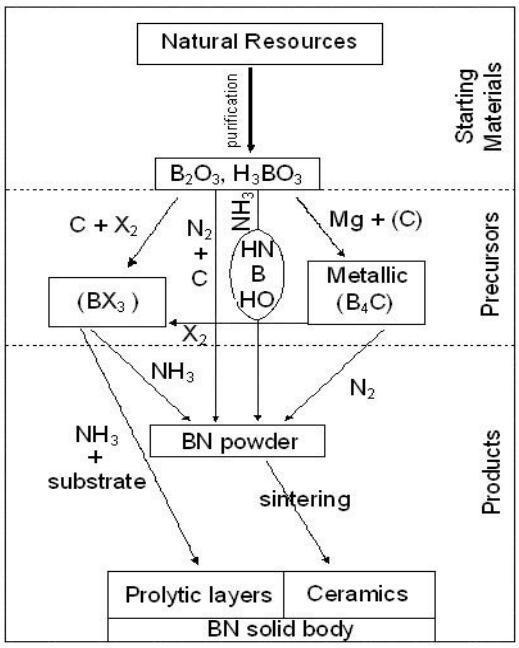

Figure 1.2. Differentiating routes of synthesis of BN.

1.1.5 Boric Acid with Ammonia

One of the hBN synthesizing method is O'Connor method which is based on the mixture of one part by weight of orthoboric acid was mixed with two parts of urea and heated under ammonia atmosphere at 1600° C (O'Connor, 1962). For all variants of description of hBN by reductive nitridation of oxidic boron compounds, boric oxide and ammonia can be considered as starting substances; these give boron nitride according to the overall equation:

$$B_2O_3 + 2NH_3 \rightarrow BN + 3H_2O$$

So-called "amide method" will be used to model the formation of hexagonal boron nitride planar networks using the ammonia – boric acid system:

According to Hubacek and Sato (1995), O'Connor method was performed in three steps. In the first step, an ammonia molecule has to approach the surface of a boric acid grain. Due to the redistribution of electron densities in the system, new bonds are created. HO-B-N-H monomer is formed and water is released as the consequence of the redistribution (Figure 1.3.). Afterwards, the monomer is stabilized by the trimerization (Figure 1.4.).

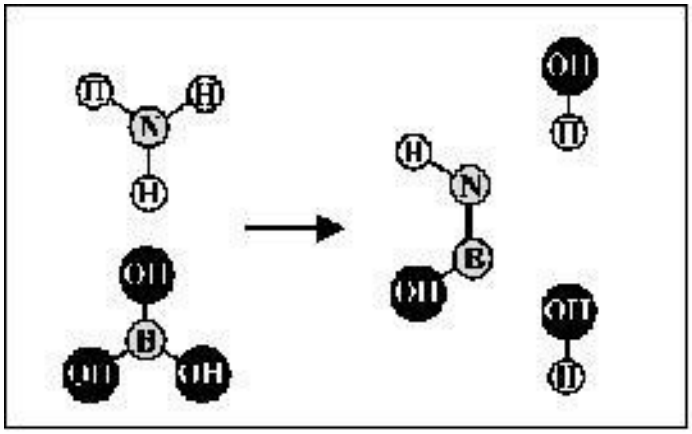

Figure 1.3. Redistribution of HO-B-N-H monomer.

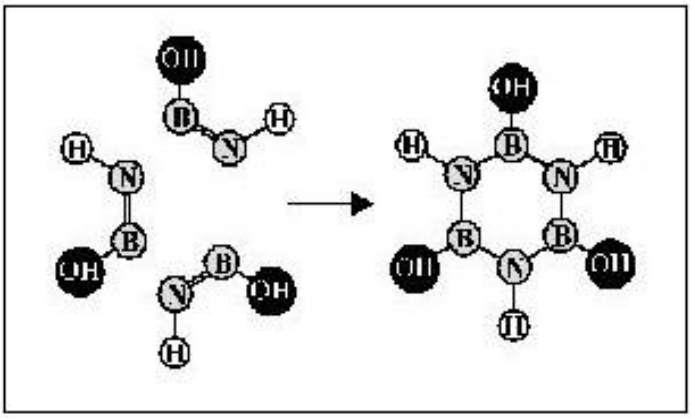

Figure 1.4. Trimerization of the monomer.

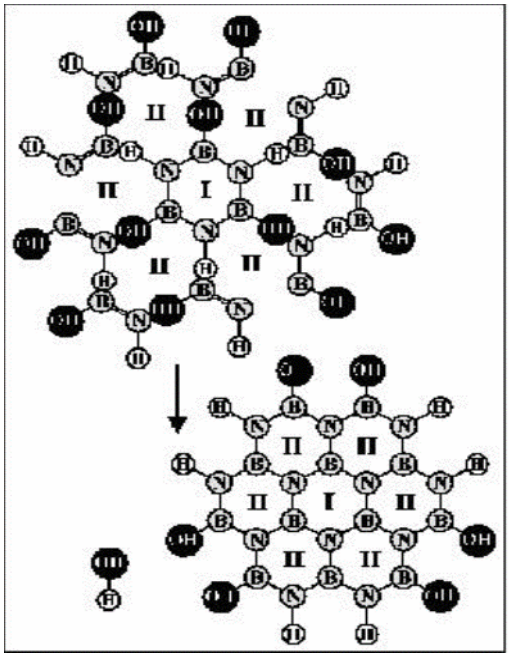

Figure 1.5. Macromolecules of BN.

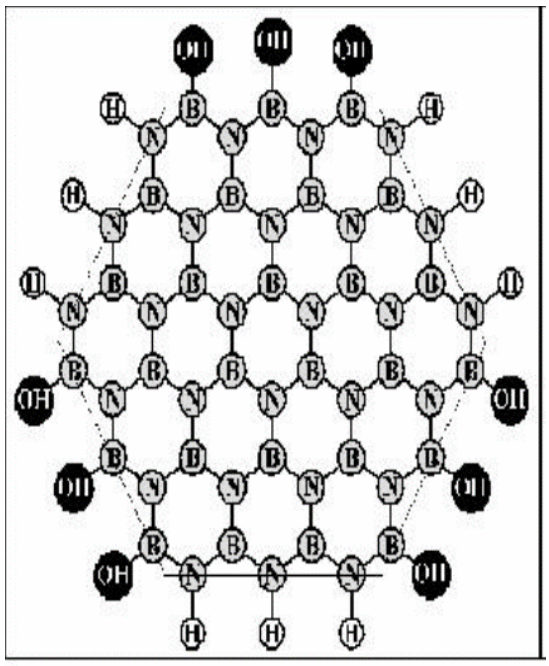

Figure 1.6. Crystalline BN.

After the third step we can get a macromolecule as shown in the Figure 1.5. The growth can continue till the size of the macromolecule reaches that which can be found in tBN powders. The size is mostly being expressed as the crystallite width, L_a, and approximately equals 10 nm. A hexagonal macromolecule with the formula HO-$B_{27}N_{27}$-H corresponds to the size.

Real crystals of BN are constructed from particular monolayers by their stacking each above other. The dipole-dipole interaction mediating stacking the layers is a chemical of the second order; so that each and every monolayer (a macromolecule) is a chemical unit of hexagonal BN. The width of the BN crystallite is then identical to the size of a macromolecule (Figure 1.6).

As shown in the previous figures, oxygen and hydrogen must not be regarded as impurities, but they represent constitutional elements terminating the two-dimensional hBN macromolecules. Since the contents of these elements are inversely proportional to the circumference-to-area ratio, it can be assumed that the larger are the BN crystals, the higher is the purity of BN. This relationship is actually the principle of the purification process, where BN is first crystallized by the thermal treatment in nitrogen gas, and oxygen impurities converted to boron oxide are washed out.

2. AIM AND SCOPE OF THE STUDY

Since hBN is engrossing material for industry in many different areas, it is used as lubricant at high temperatures, in space applications as an insulator for electronics, and radiation shielding material.

The aim of this thesis is to synthesize hBN in the presence of metal oxides at optimal temperatures and to characterize samples by FTIR, XRD and SEM.

The effect of metal oxide additives on the formation of hBN will be determined, and identification of synthesized samples will be examined. In brief, objectives of this study are substance as follows:

To determine the effect of type of metal oxide,

To improve crystallinity of hBN,

To reduce the synthesis temperature of hBN,

To increase the grain size of hBN,

To compare grain size of hBN with different metal oxides,

To investigate the morphology of hBN samples in nanoscale.

3. EXPERIMENTALS

3.1 Chemicals

Boron oxide (Fluka, 97%), urea (Fluka, 99%), barium oxide (Aldrich, 97%), calcium oxide (Aldrich, 99.99%), chromium(III) oxide (Aldrich, 98%), lanthanum(III) oxide (Alfa Aesar, 99.9%), lithium oxide (Aldrich, 97%), magnesium oxide (Merck, 98%), scandium(III) oxide (Abcr, 99.9%), sodium oxide (Aldrich, 80%), vanadium(V) oxide (Aldrich, 99.6%), yttrium(III) oxide (Abcr, 99.99%), zinc oxide (Merck, 99%), zirconium(IV) oxide (Alfa Aesar, 99%), ethanol (Merck, 99.5%) and hydrochloric acid (Merck, 37%) were commercially obtained and used without any purification.

3.2 Synthesis of hBN Samples

Synthesis of hBN compounds were carried out with modified O'Connor method. The mixture of 1 g boron oxide 2 g of urea and 0.6 g of metal oxides (BaO, CaO, Cr_2O_3, La_2O_3, Li_2O, MgO, Sc_2O_3, Na_2O, V_2O_5, Y_2O_3, ZnO and ZrO_2) were mixed and powdered with a mortar and a pestle. Followed by the mixture was pre-heated at 200°C for 2 hours in furnace to obtain precursor. Then the precursor re-powdered in mortar and heated in tube furnace under ammonia atmosphere (with a flow rate of 120 mL/min) at different temperatures (1000°C, 1150°C, 1300°C and 1450°C) for 3 hours.

Finally, the product was boiled in 9.1% HCl solution then filtrated in hot water (500 mL) and ethanol respectively and dried in oven at 100°C then bottled.

3.3 Preparation of hBN Samples

3.3.1 Agate Mortar and Pestle

The mixture of boron oxide, urea and additive oxide were powdered and homogenized in agate mortar and pestle for 20 minutes.

Figure 3.1. Agate mortar and pestle.

3.3.2 Camera Furnace

The pulverized mixture located in a beaker was heated to obtain precursor in Protherm PLF 140/5 camera furnace at 200°C for 2 hours.

Figure 3.2. Protherm PLF 140/5

3.3.3 Tube Furnace

The main heating was done with Protherm PTF 15/75/450 tube furnace (average heating rate: 7°C/min) at different temperatures (1150°C, 1300°C and 1450°C) under ammonia atmosphere (flow rate 120 mL/min) for 3 hours.

Figure 3.3. Protherm PTF 15/75/450

3.4 Characterization of hBN Samples

3.4.1 FTIR Spectroscopy

FTIR spectrum analysis of hBN samples were recorded with Perkin Elmer Spectrum Two IR Spectrometer in a range between wavelengths of 400-4000 cm^{-1}.

Figure 3.4. Perkin Elmer Spectrum Two IR Spectrometer

3.4.2 XRD Measurement

XRD diffractogram of hBN samples were done with Rigaku Multiflex diffractometer using CuK_{α} radiation. (40 kV / 30 mA, Goniometer: MultiFlex+ goniometer (with a shutter), Div Slit: ½ deg., Sct Slit: ½ deg., Rec Slit: 0.15 mm, Scan Speed: 5 deg / min., Attachment: Standard sample holder)

Figure 3.5. Rigaku Multiflex diffractometer

3.4.3 SEM Analysis

SEM images were obtained by Jeol JSM 6390LV. Before SEM analysis, the samples were coated with gold for 220 seconds at 4mA by using Coxem KIC-1A ION-COATER.

Figure 3.6. Jeol JSM 6390LV

Figure 3.7. Coxem KIC-1A ION-COATER

3.5 Sample Calculations

3.5.1 Calculation of Lattice Parameters

Lattice parameters of the samples were calculated by using Equation 1 for hexagonal systems.

$$\frac{1}{d^2} = \frac{4}{3} \times \left[\frac{h^2 + hk + k^2}{a^2}\right] + \frac{l^2}{c^2} \qquad (1)$$

d : Interlayer spacing

h, k, l : Related Miller indices

a, c : Lattice parameter

Calculation of "a" parameter of hBN:
For 110 peak of hBN d is 1.250 Å

$$\frac{1}{(1.250)^2} = \frac{4}{3} \times \frac{1^2+1\times1+1^2}{a^2} + \frac{0^2}{c^2}$$

a = 2.500 Å

Calculation of "c" parameter of hBN:
For 002 peak of hBN d is 3.306 Å

$$\frac{1}{(3.306)^2} = \frac{4}{3} \times \frac{0^2+0\times0+0^2}{a^2} + \frac{2^2}{c^2}$$

a = 6.612 Å

3.5.2 Calculation of Grain Size

Scherrer equation (Equation 2) relates the peak breadth of a specific phase of a material to the mean crystallite size of that material.

$$L = \frac{K\lambda}{\beta \cos\theta} \qquad (2)$$

β is the difference of the width of the peak at half maximum intensity of a specific phase (hkl) in radians of reference material and sample.

K is a constant that varies with the method of taking the breadth (0.9).

λ is the wavelength of incident X-Rays (CuK_{α}=1.504 Å).

2θ is the center angle of the peak of sample

L is the crystallite size

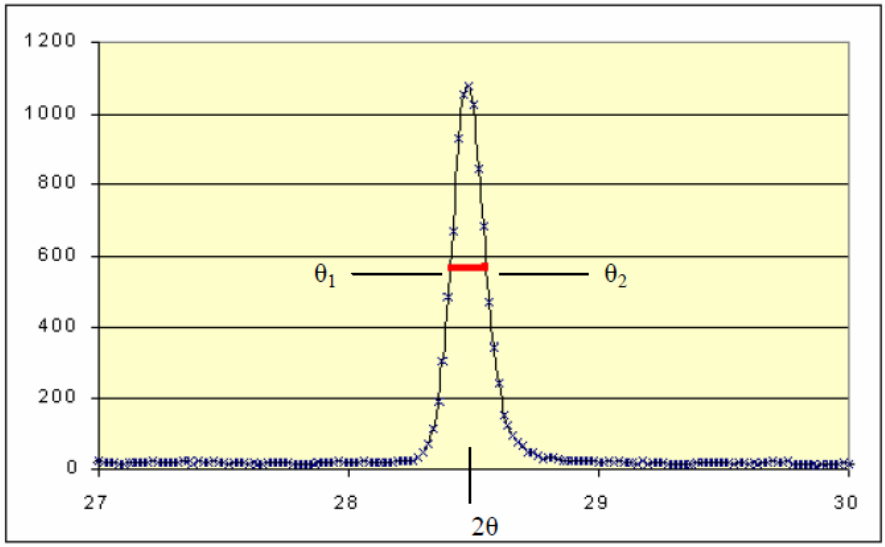

$\theta_{Ref.1}$ (26.64°) and $\theta_{Ref.2}$ (26.97°) are angles of the width of the peak at half maximum intensity in radians of reference material. $\theta_{Samp.1}$ (25.94°) and $\theta_{Samp.2}$ (26.97°) are angles of the width of the peak at half maximum intensity in radians of sample and 2θ is 26.54° for sample.

$$\beta = \sqrt{\left((26.97 - 26.64) \times \frac{\pi}{180}\right)^2 - \left((26.97 - 26.64) \times \frac{\pi}{180}\right)^2}$$

$$\beta = 0.02$$

$$L = \frac{K\lambda}{\beta \cos\theta} = \frac{0.9 \times 1.504}{0.02 \times \left(\cos\left[13.27 \times \frac{\pi}{180}\right)\right]}$$

$$L = 92.4 \text{ Å}$$

$$L = 9.24 \text{ nm}$$

3.5.3 Calculation of graphitization index

The degree of crystallization of the hBN phase was appraised in terms of the "graphitization index" (G.I.) as three dimensional order is the ratio of (102) into the (100) and (101) directions (Balint and Petrescu, 2009; Thomas et al, 1962), as

$$G.I = \frac{Area(100) + Area(101)}{Area(102)}$$

4. RESULTS & DISCUSSION

The modified O'Connor method was used to synthesize boron nitride for because it is the simplest method to form hBN with using easily purchasable chemicals and devices besides without using expensive laboratory devices (Budak, 1999).

The characterization of structure and formation of hBN firstly introduced by IR spectroscopy. The IR spectrum of hBN includes three main absorption peaks at ~3550, ~1430 and, ~780 cm^{-1}. The ~1430 and ~780 peaks specifies the in-plane and out-plane B-N vibrations of hBN respectively. The in-plane and out-of-plane vibrations are very close to the literature (Hubacek et al, 1994). Also the ~1050 cm^{-1} and ~3550 cm^{-1} peak refers to the B-O and O-H stretching vibration respectively. The B-O vibrations are observed as a shoulder peak.

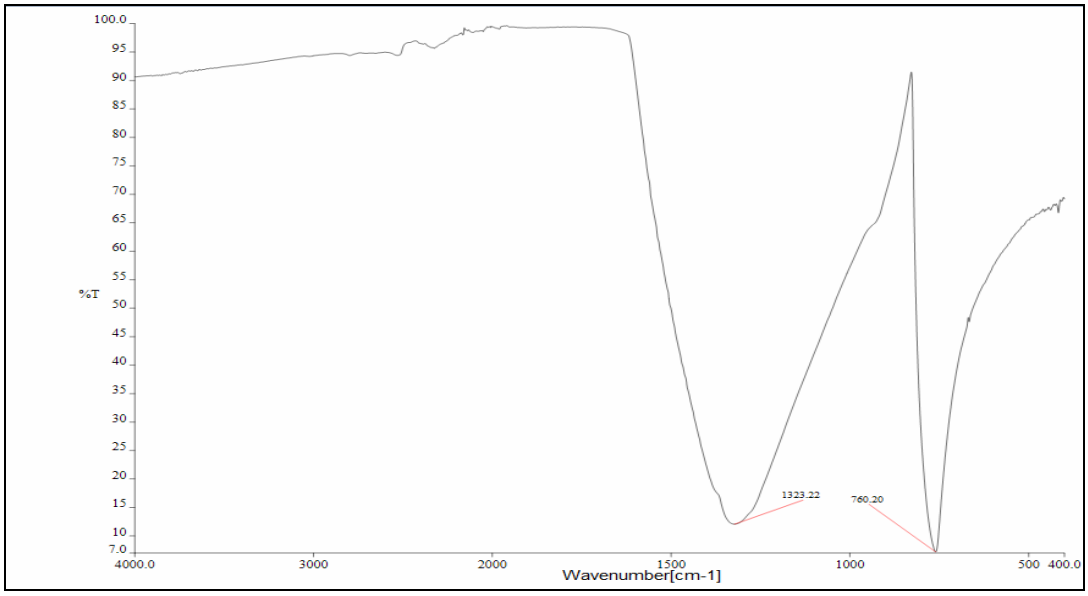

Figure 4.1. FTIR spectrum of hBN in presence of BaO at 1450°C

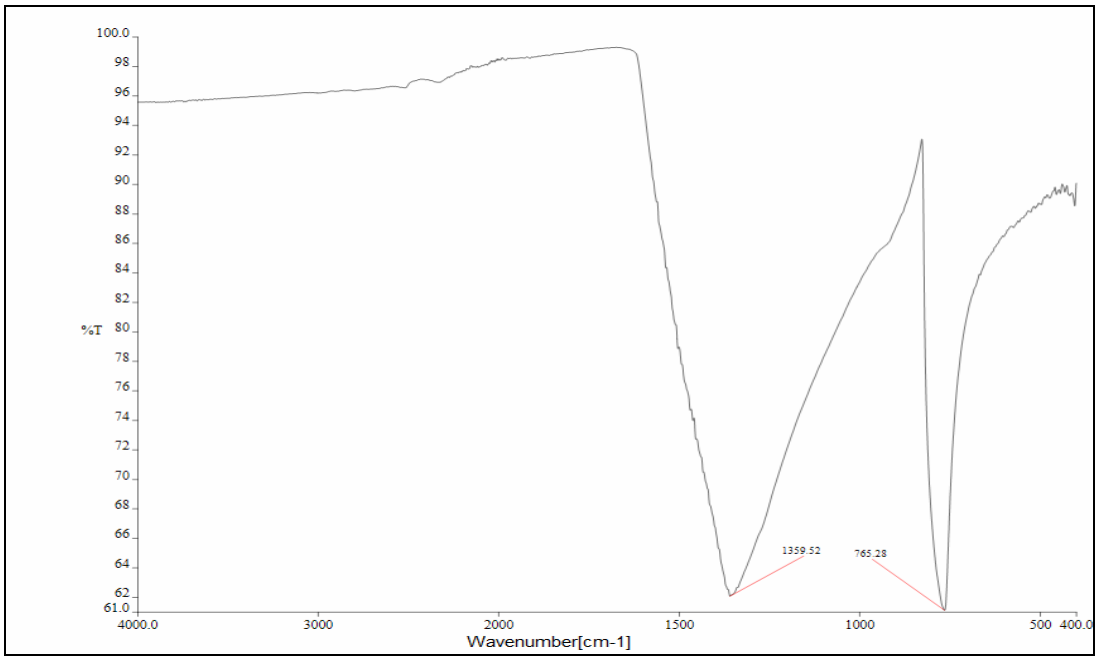

Figure 4.2. FTIR spectrum of hBN in presence of Li_2O at 1450°C

As it is shown in the Figure 5.1 and Figure 5.2 (see Appendix A for all FTIR spectra of hBN samples), the peaks at ~1430 and ~780 cm-1 of hBN IR spectra are very close to the literature.

The information about crystallinity of hBN is obtained from XRD analysis. The results were compared with standard hBN (ICDD card no: 34 – 421). The main peaks of hBN (002, 100, 101, 102, 004, 110, 112, and in some diffractograms 103, 104 and 006) are observed (see Appendix B for all XRD diffractograms of hBN samples).

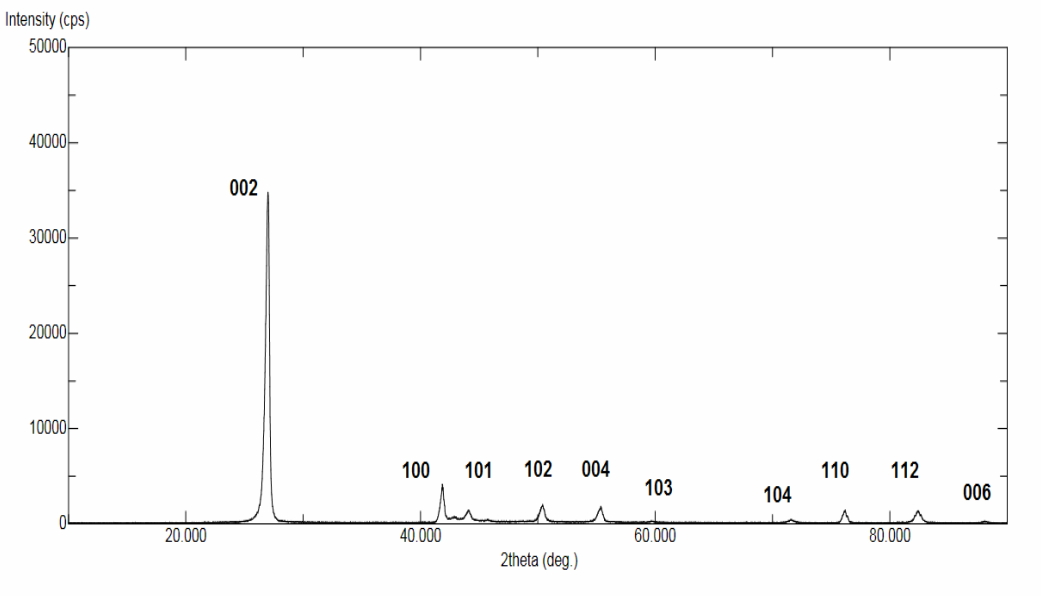

Figure 4.3. XRD pattern of hBN in presence of BaO.

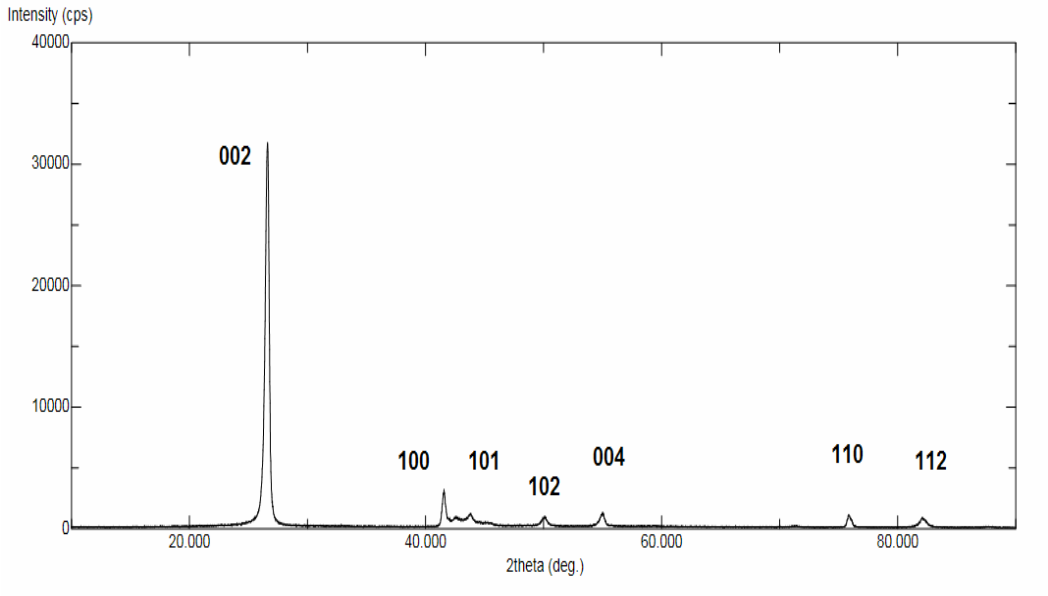

Figure 4.4. XRD pattern of hBN in presence of MgO.

The interlaying distances calculated from XRD based on different temperatures with different metal oxides are shown in Table 4.1.

Table 4.1 Interlayer distance of hBN samples in presence of metal oxides at different temperatures.

Synthesis Temperature	Used Oxides	2θ	*d*
1450℃	BaO	26.999	3.300
	CaO	26.704	3.335
	Cr_2O_3	N.D.	N.D.
	La_2O_3	26.780	3.326
	Li_2O	26.802	3.324
	MgO	26.599	3.348
	Na_2O	26.942	3.307
	Sc_2O_3	26.825	3.321
	V_2O_5	26.776	3.327
	Y_2O_3	26.798	3.324
	ZnO	26.728	3.333
	ZrO_2	26.784	3.326
1300℃	BaO	26.920	3.309
	CaO	26.763	3.328
	La_2O_3	26.848	3.318
	Li_2O	26.849	3.318
	MgO	26.905	3.311
1150℃	Li_2O	26.951	3.306
1000℃	Li_2O	26.886	3.313

N.D.; Not Detected

The lattice parameters of hBN samples were calculated (Table 4.2) from the XRD patterns show proximity with the literature values (ICDD card no: 34 – 421, a= 2.5044 Å, c= 6.6565 Å, d= 3.3281 Å).

Table 4.2 Calculated lattice parameters of metal oxides in different temperatures.

Synthesis Temperature	Used Oxides	Lattice Parameters (Å)		
		a	c	d
1450 °C	BaO	2.498	6.600	3.300
	CaO	2.506	6.670	3.335
	Cr_2O_3	N.D.	N.D.	N.D.
	La_2O_3	2.498	6.652	3.326
	Li_2O	2.502	6.648	3.324
	MgO	2.506	6.696	3.348
	Na_2O	2.496	6.614	3.307
	Sc_2O_3	2.496	6.642	3.321
	V_2O_5	2.484	6.654	3.327
	Y_2O_3	2.500	6.648	3.324
	ZnO	2.520	6.652	3.330
	ZrO_2	2.520	6.652	3.326
1300 °C	BaO	2.500	6.618	3.309
	CaO	2.500	6.656	3.328
	La_2O_3	2.498	6.636	3.318
	Li_2O	2.502	6.636	3.318
	MgO	2.496	6.622	3.311
1150 °C	Li_2O	2.500	6.612	3.306
1000 °C	Li_2O	2.498	6.626	3.313

N.D.; Not Detected

The broadening in the XRD peaks testifies that the particle size of the samples is within nanometer scale. The grain size of hBN are calculated (Table 4.3) by using the Scherrer equation.

Table 4.3 Calculated average grain size of hBN in presence of metal oxides in different temperatures.

Synthesis Temperature	Used Oxides	Average Grain Size (nm)
1450 °C	BaO	39.97
	CaO	54.33
	Cr_2O_3	N.D.
	La_2O_3	12.53
	Li_2O	51.44
	MgO	38.63
	Na_2O	30.67
	Sc_2O_3	14.75
	V_2O_5	13.72
	Y_2O_3	21.17
	ZnO	16.93
	ZrO_2	8.67
1300 °C	BaO	80.22
	CaO	21.94
	La_2O_3	17.78
	Li_2O	43.37
	MgO	11.99
1150 °C	Li_2O	334.80
1000 °C	Li_2O	23.12

N.D.; Not Detected

The graphitization indexes of hBN samples were calculated with the G.I. formula (Table 4.4)

Table 4.4 Calculated average grain size of hBN in presence of metal oxides in different temperatures.

Synthesis Temperature	Used Oxides	Graphitization Index
1450℃	BaO	2.80
	CaO	2.77
	Cr_2O_3	N.D.
	La_2O_3	N.D.
	Li_2O	N.D.
	MgO	4.97
	Na_2O	N.D.
	Sc_2O_3	N.D.
	V_2O_5	N.D.
	Y_2O_3	N.D.
	ZnO	N.D.
	ZrO_2	N.D.
1300℃	BaO	4.52
	CaO	5.35
	La_2O_3	N.D.
	Li_2O	2.25
	MgO	N.D.
1150℃	Li_2O	1.75
1000℃	Li_2O	N.D.

N.D.; Not Detected

Boron nitride was not considered crystalline for practical purposes when the interlayer spacing is greater than 0.335 nm and the crystallites smaller than 50 nm (Budak and Bozkurt, 2004). In present study, SEM micrographs of the h-BN in the presence of metal oxides [M=Ba, Ca, Cr, La, Li, Mg, Na, Sc, V, Y, Zn, Zr] are examined (Figure 5.5 and Figure 5.6). These samples are crystalline as they can be clearly seen from their XRD patterns. Since the crystallinity information can be obtained by XRD diffractograms, the SEM analysis were supported the nano structures of synthesized materials with only surface appearance.

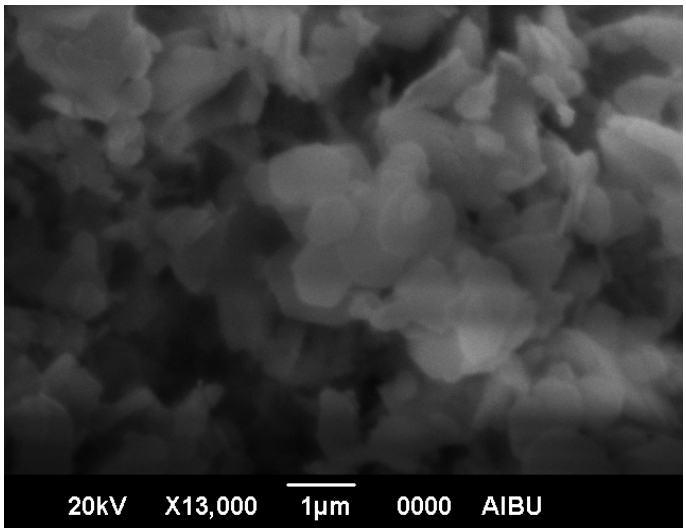

Figure 4.5. Sample SEM image of hBN in presence of BaO.

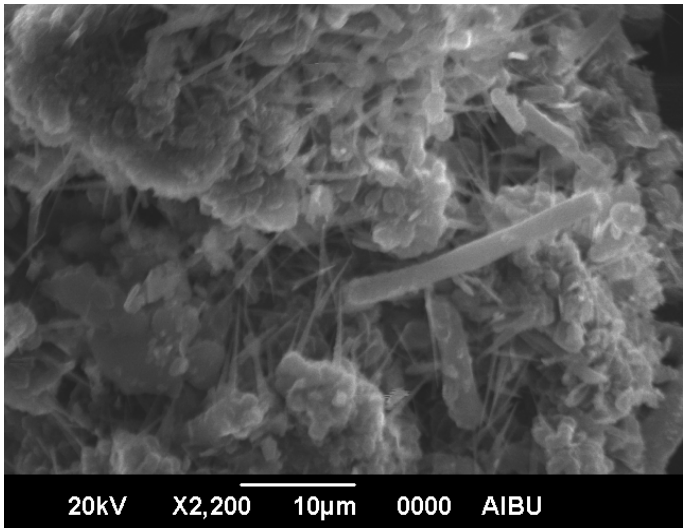

Figure 4.6. Sample SEM image of hBN in presence of Li_2O.

The study was pointed out that metal oxides play an important role in the crystallization of h-BN. In the study the metal oxides were used as fluxing agent. It is known that the hexagonal form of boron nitride can not be obtained below 1700°C, when it is synthesized according to the O'Connor method. On the other hand, metal oxides [M=Ba, Ca, Cr, La, Li, Mg, Na, Sc, V, Y, Zn, Zr] addition to the precursor mixtures decreases crystallization temperature.

The decrease of crystallization temperature arises by the metal oxide additions prevents the boron oxide to melt homogeneously, and provide the boron atom to bond with nitrogen atom at lower temperature. Since the melting point of boron oxide is 450°C, and the additive causes boron oxide to melt at lower temperature and easing the bonding of boron and nitrogen.

The well-known peaks of hBN (002, 100, 101, 102, 004, 110, and 112) were observed in most of the sample XRD diffractograms. Besides, the inseparable (100) and (101) XRD peaks of hBN causes the product to be accepted as turbostratic according to previous studies and also resulting the crystallinity very low. Whereas the G.I formula is based on those peaks, inseparable (100) and (101) peaks prevents the G.I calculation.

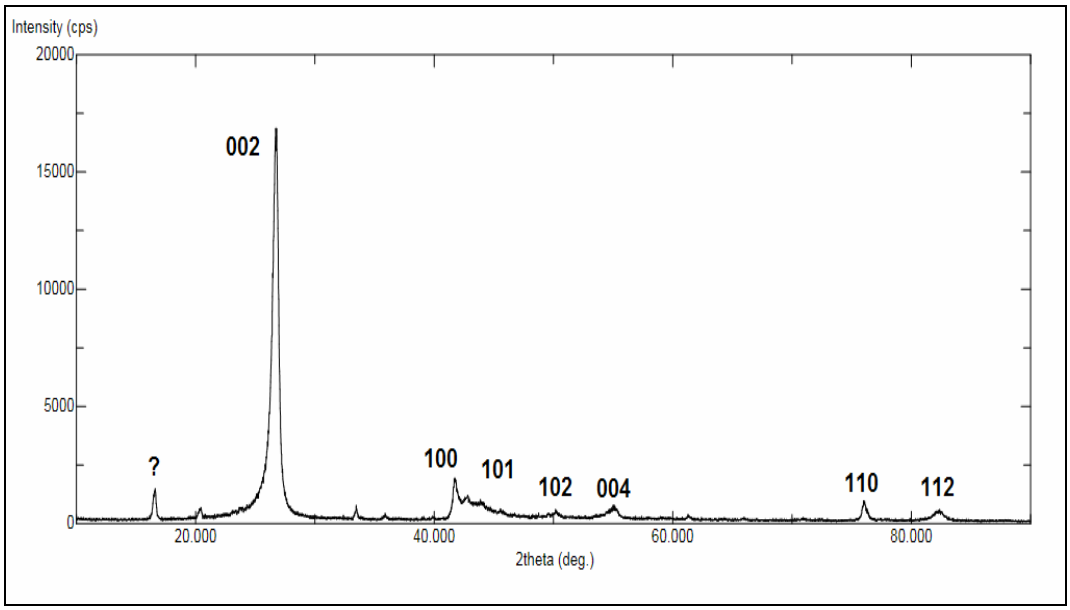

Figure 4.7 XRD pattern of hBN in presence of ZnO at 1450°C

The additive percentage effects the hBN formation because the reaction surface area and reduction in molten phase for a long time or reductive properties of fluxes. According to previous studies (Oz, 2013), the addition of more than 20% enhances the hBN formation. Besides, high amount of additives might prevent the interaction between nitrogen and boron containing compounds.

There are three main oxide types used in this study, which can be classified as angled (Li_2O and Na_2O), linear (MgO, CaO, BaO and ZnO) and bridging (Sc_2O_3, Y_2O_3, La_2O_3, V_2O_5, Cr_2O_3, ZrO_2). The metal oxides with bridging oxygen have higher lattice energy, and increasing period number brings decreasing covalent character and increasing ionic character because of increasing metallic character. In addition, the higher lattice energy cause higher melting point. XRD patterns show clearly, that metal oxides with bridging oxygen are unproductive for this kind of synthesis. Among used oxides, the most efficient oxide types are found as linear (CaO and BaO) and angled (Li_2O).

An allegation is arised in previous studies (Budak and Bozkurt, 2004; Yucel 2005), that there is an electronic interactions between the metal atom and hBN, d-π interaction. Increasing valance electron in metal increases interaction with π orbital of BN and causes decreasing interlaying spacing. However, results show that neither atomic size nor coordination number of metal atoms have no significant effect on the formation of hBN, metals with relatively high coordination number used in the first place. But the interlaying distance is observed to be dependent on the synthesis temperature where the lower temperature causes lower interlaying spacing.

The hBN formations were also determined at high temperatures such as 1450°C. But lithium salts as in the previous studies (Oz, 2013), the lithium oxide addition in present study is increased the crystallinity of hBN even low temperatures such as 1300°C and 1150°C. In XRD diffractogram of hBN sample in presence of Li_2O at 1300°C and 1150°C (104) peak was observed which indicates the higher crystallinity (Figure 5.8 and Figure 5.9).

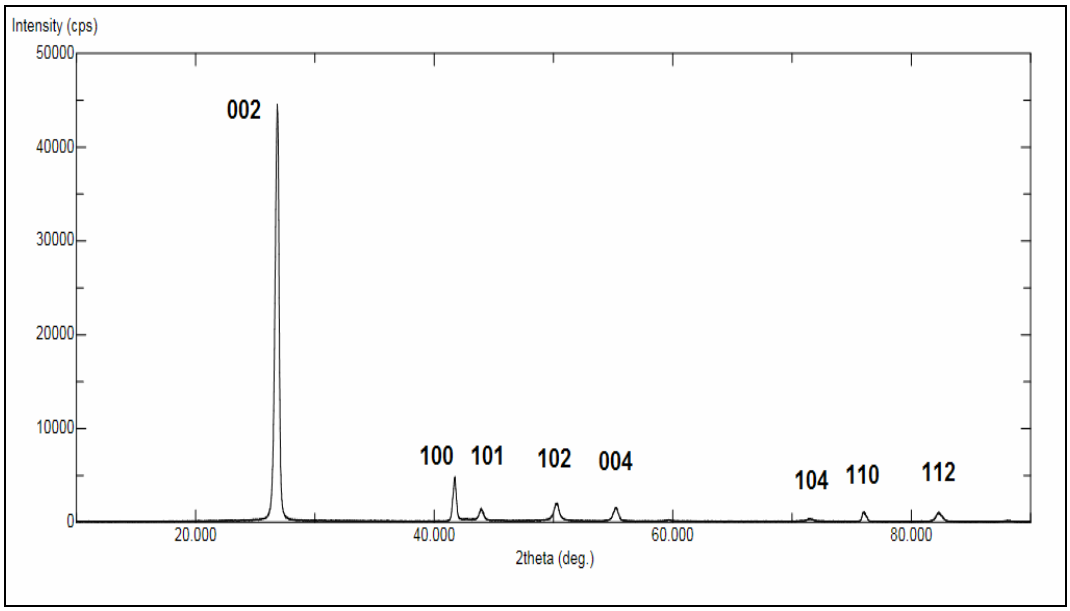

Figure 4.8. XRD pattern of hBN in presence of Li_2O at 1300°C

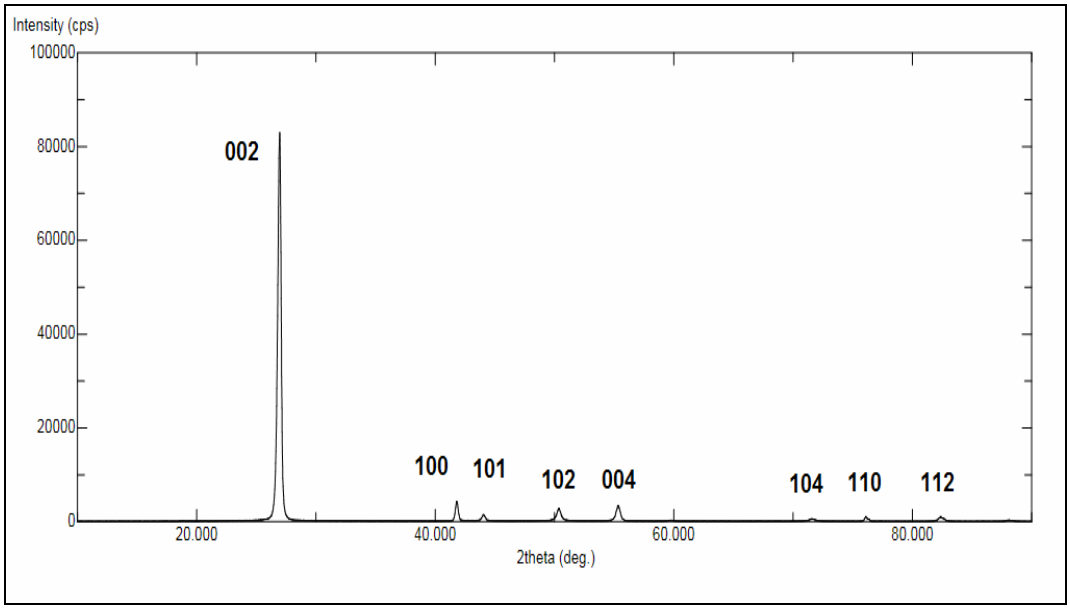

Figure 4.9. XRD pattern of hBN in presence of Li_2O at 1150°C

All SEM image explications were based on Shimomura (Shimomura et al, 1995). The results indicate that the grains are irregular shape and order. Plate-like, web-like and needle-like structures were observed. However, the distribution of these structure images were irregular and not homogeneous. In addition, gold coated hBN

samples on SEM sample disc was thin-layered, as the increasing SEM accelerations for magnifying the image, the specimens had distortions and some of the well-crystallized samples seen on XRD pattern could not be observed as plate-like, web-like or needle-like structures (Figure 5.10).

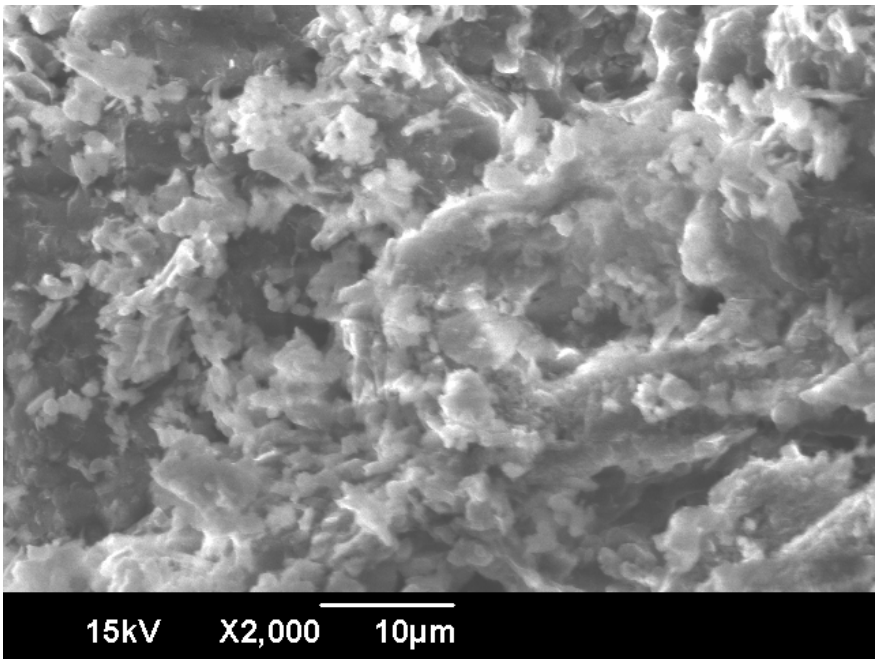

Figure 4.10. SEM image of hBN in presence of Li_2O at 1300°C with distorted specimen.

As a result, hBN samples were prepared at relatively at low temperature and formation of B-N confirmed by FTIR. Not every used metal oxides was experimented at all low temperatures. Since their XRD patterns showed the low crystallinity, lowering the temperature of these metal oxides was not necessary. The grain size of hBN samples and calculated lattice parameters were very close to reported value of original hBN.

5. CONCLUSION

In summary, hBN samples were prepared with the modified O'Connor method at different temperatures under ammonia atmosphere and following conclusions can be stated:

1. FTIR investigations confirm the formation hBN.
2. XRD patterns of the samples are indexed as hBN and calculated lattice parameters are very close to reported values of hBN.
3. The broadening nature of the XRD peaks indicates that the particle size of the samples is within nanometer scale.
4. Usages of metal oxides permit lowering the formation temperature of hBN. Addition, usages of metal oxides cause the formation of the nano structures occur at low temperature such as 1300°C and 1150°C.
5. Among used oxides, the most efficient oxide types are found as linear (CaO and BaO) and angled (Li_2O). Metal oxides with bridging oxygen was found to be unproductive.
6. An electronic interaction between the metal atom and hBN, d-π interaction, is questionable.
7. Interlaying spacing of hBN samples are found to be dependent on the temperature. Decreasing temperature, lowers the interlaying spacing.
8. The nanoscale hBN samples were synthesized and plate-like, web-like and needle-like formations were observed in hBN samples.
9. It was possible to obtain high crystalline hBN powder at lower temperature such as 1150°C, which would be sufficient temperature for commercial applications.

6. REFERENCES

Balint MG and Petrescu MI (2009) "An attempt on identify the presence of polytype stacking faults in hBN powders by means of X-Ray diffraction", *Diamond and Related Materials,* 18: 1157-1162.

Balmain WH (1842) "Bemerkungen über die Bildung von Verbindungen des Bors und Siliciums mit Stickstoff und gewissen Metallen", J Prakt Chem., 27: 422-430.

Budak E and Bozkurt Ç (2004) "The effect of transition metals on the structure of h-BN intercalation compounds", J. Solid State Chem. 177: 1768-1770.

Budak E (1999) The synthesis and modification of hexagonal boron nitride, MSc Thesis, AİBÜ Graduate School of Natural and Applied Sciences, Bolu.

Chamber of Mining Engineers of Turkey, Boron Report, http://www.maden.org.tr/resimler/ekler/6358599b7afb250_ek.pdf?tipi=5&turu=R&sube=0, 18 June 2015.

Choi JY, Kang SJL, Fukanaga O, Park JK and Eun KY (1993) "Effect of B_2O_3 and hBN Crystallinity on cBN Synthesis", *Journal of American Ceramic Society* 76 (10): 2525-2528.

Haubner R, Wilhelm M, Weissenbacher R and Lux B (2002) "Boron Nitrides-Properties, Synthesis and Applications. In: Jansen, M. (ed). HighPerformance Non- Oxide Ceramics II. 15. Springer Verlag. Berlin.

Hubacek M and Sato T (1995) "Preparation and properties of a compound in the B-C-N system", J. Solid State Chem., 114: 258-264.

Hubacek M, Sato T and Ishi T (1994) "A Coexistance of Boron Nitride and Boron Oxide", J. Solid State Chem. 109: 384-390.

Hubacek M, Sate T and Ueki M (1997) "Copper-boron nitride interaction in hot-pressed Ceramics" J. Mater. Res., 12 (1): 113-118.

Hubacek M and Ueki M (1996) "Chemical Reactions in Hexagonal Boron Nitride System" *Journal of Solid State Chemistry* 123: 215-222.

Hubacek M, Ueki M and Brozek V (1996) "Hypothetical model of turbostratic layered boron nitride", J. Ceramic Society of Japan, 104 [8]: 695-698.

Lipp A, Schwetz KA and Hunold K (1989) "Hexagonal boron nitride: fabrication, properties and applications", Journal of the European Ceramics Society, 5: 3–9.

O'Connor TE (1962) "Synthesis of Boron Nitride", J. Am. Chem. Soc. 84: 1753-1754.

Öz M (2013) Synthesis of hexagonal boron nitride in the presence of fluxing agents, PhD Thesis, AİBÜ Graduate School of Natural and Applied Sciences, Bolu.

Petrescu MI and Balint MG (2007) "Structure and properties modifications in boron nitride. Part I: Direct polymorphic transformations mechanisms" U.P.B. Sci. Bull., Series B, 69 (1): 35-42.

Shimomura J, Funahashi T and Koitabashi T (1995) "Electron Microscopy of Hexagonal Boron Nitride Powder", J Mater Sci. 30: 3193- 3199.

Thomas J, Weston NE and O'Connor TE (1962) "Turbostratic Boron Nitride, Thermal Transformation to Ordered-layer-lattice Boron Nitride", *Journal of American Chemistry Society* 84: 4619-4622.

Yücel N (2005) Effect of metal carbonyls on the formation of hexagonal boron nitride, MSc Thesis, AİBÜ Graduate School of Natural and Applied Sciences, Bolu.

APPENDICES

7. APPENDICES

Appendix A. FTIR Spectra of hBN Samples

Appendix A.1. FTIR Spectra of hBN Samples at 1450°C

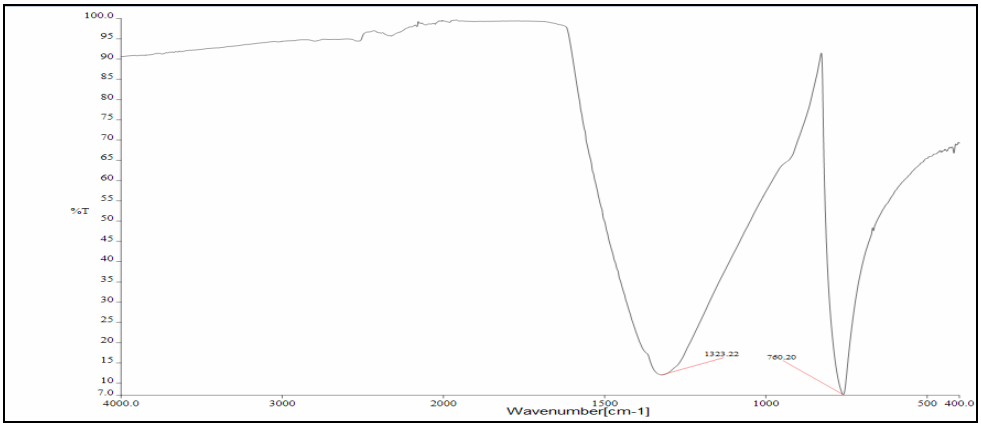

Figure A.1.1. FTIR spectrum of hBN in presence of BaO 1450°C.

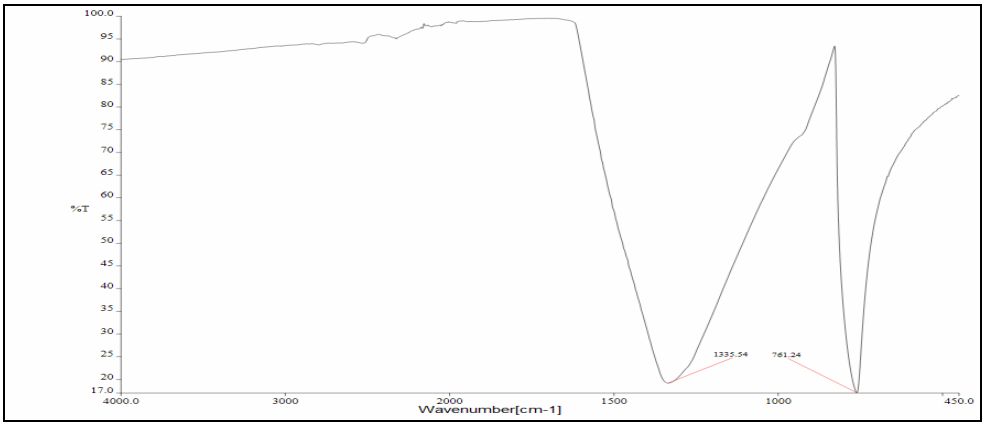

Figure A.1.2. FTIR spectrum of hBN in presence of CaO 1450°C.

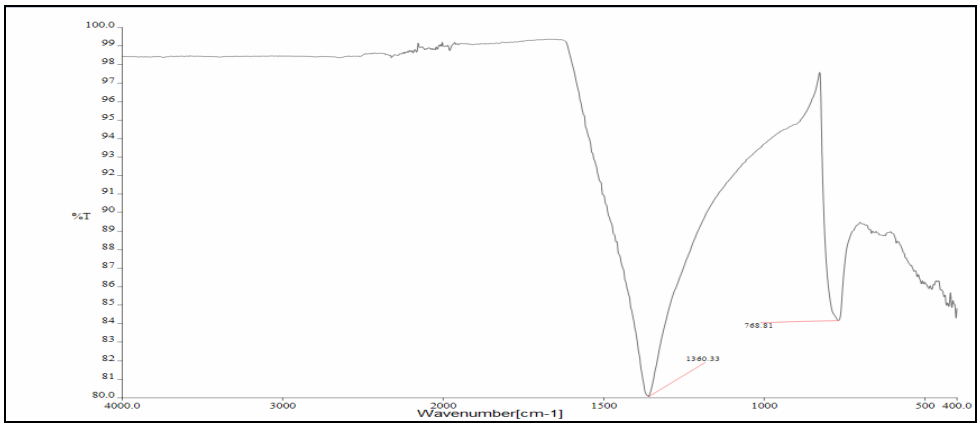

Figure A.1.3. FTIR spectrum of hBN in presence of Cr_2O_3 1450°C.

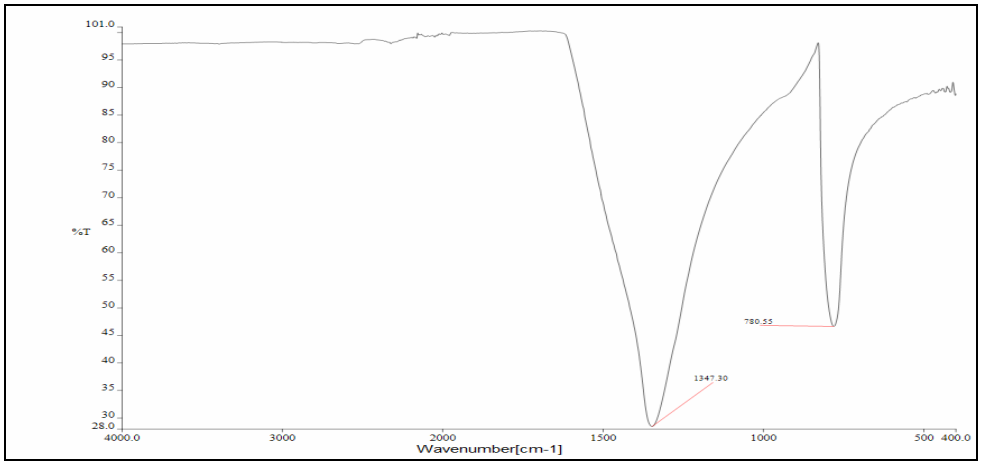

Figure A.1.4. FTIR spectrum of hBN in presence of La_2O_3 1450°C.

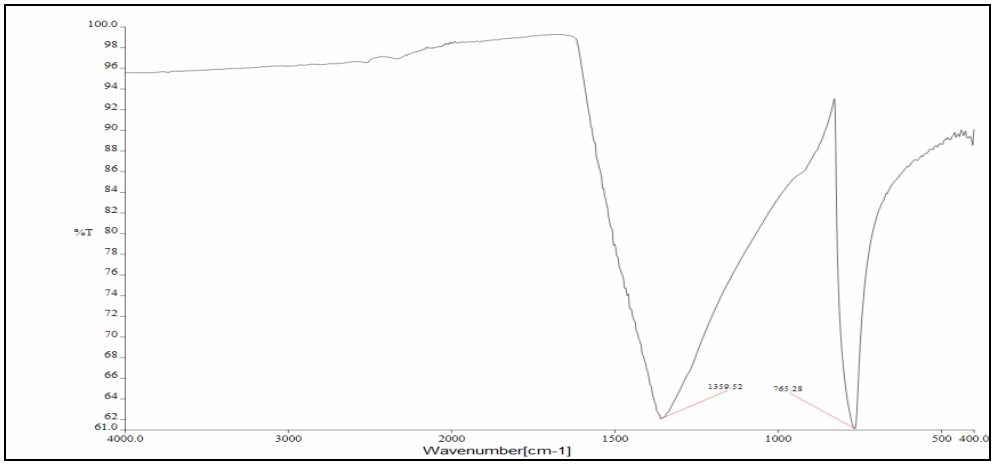

Figure A.1.5. FTIR spectrum of hBN in presence of Li_2O 1450°C.

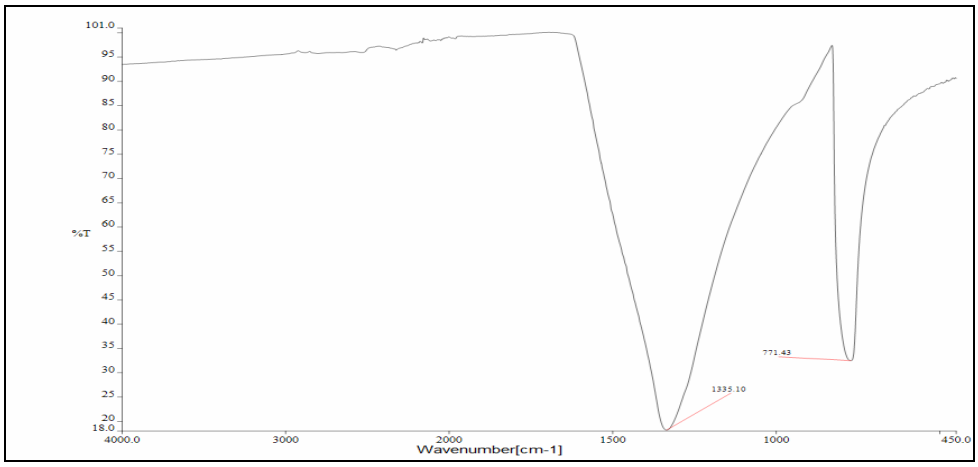

Figure A.1.6. FTIR spectrum of hBN in presence of MgO 1450°C.

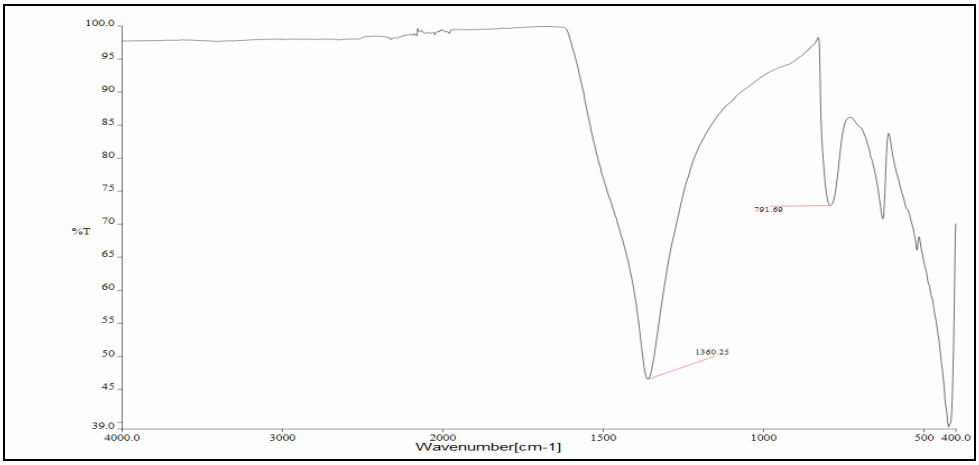

Figure A.1.7. FTIR spectrum of hBN in presence of Sc_2O_3 1450°C.

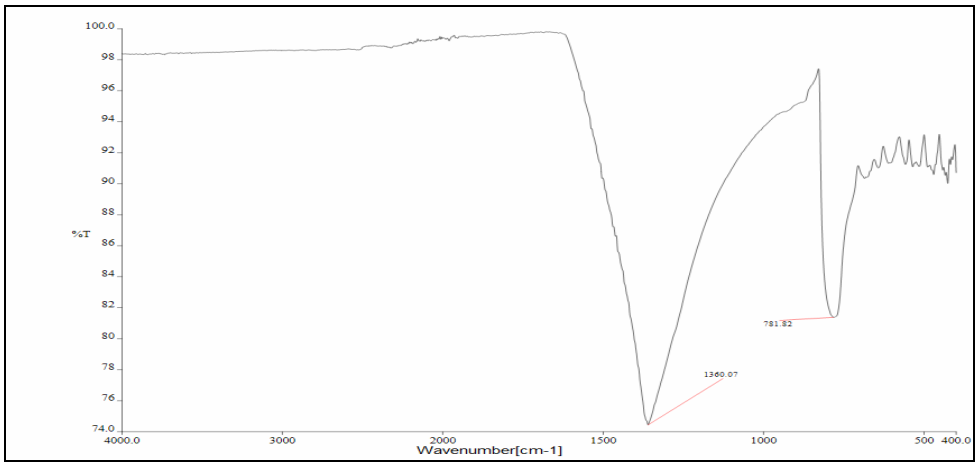

Figure A.1.8. FTIR spectrum of hBN in presence of Na_2O 1450°C.

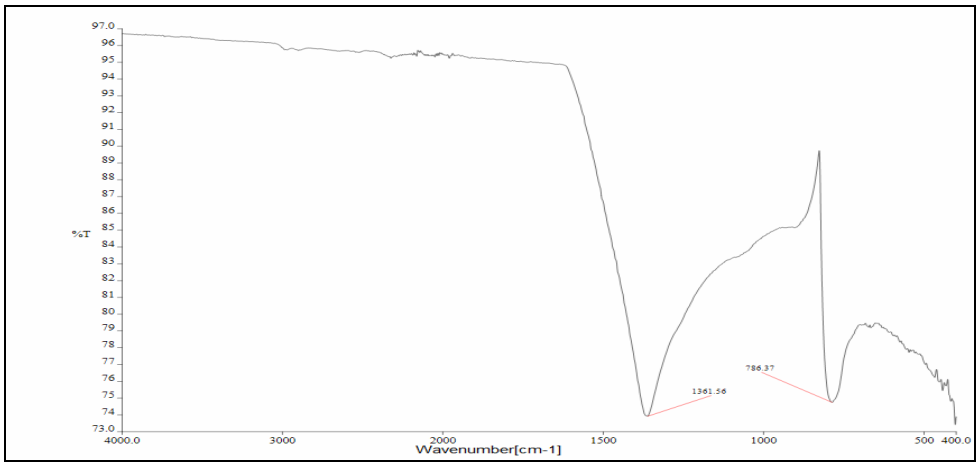

Figure A.1.9. FTIR spectrum of hBN in presence of V_2O_5 1450°C.

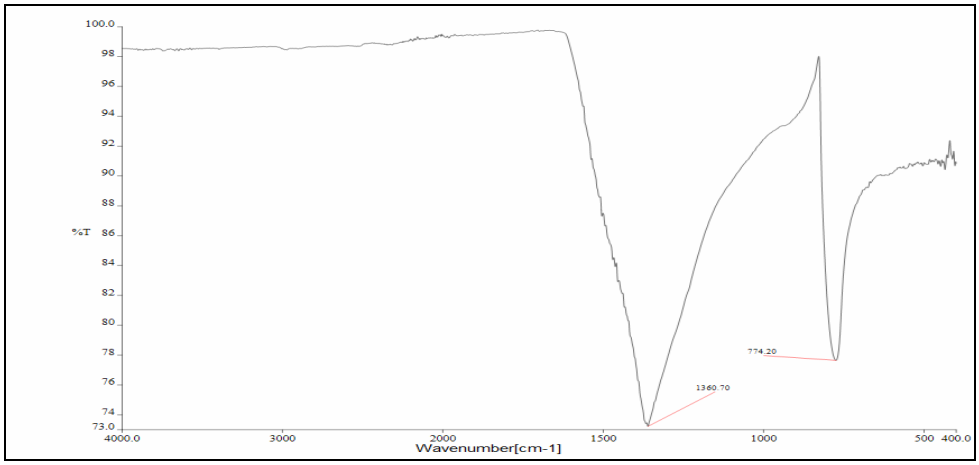

Figure A.1.10. FTIR spectrum of hBN in presence of Y_2O_3 1450°C.

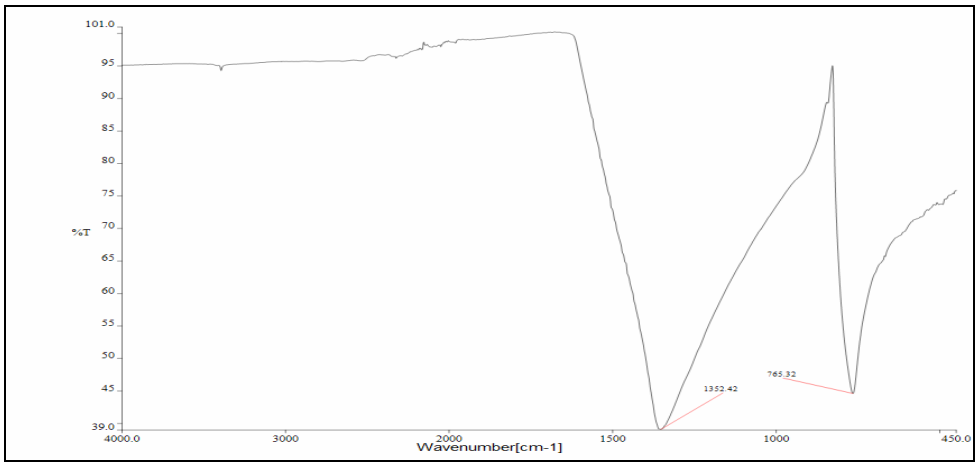

Figure A.1.11. FTIR spectrum of hBN in presence of ZnO 1450°C.

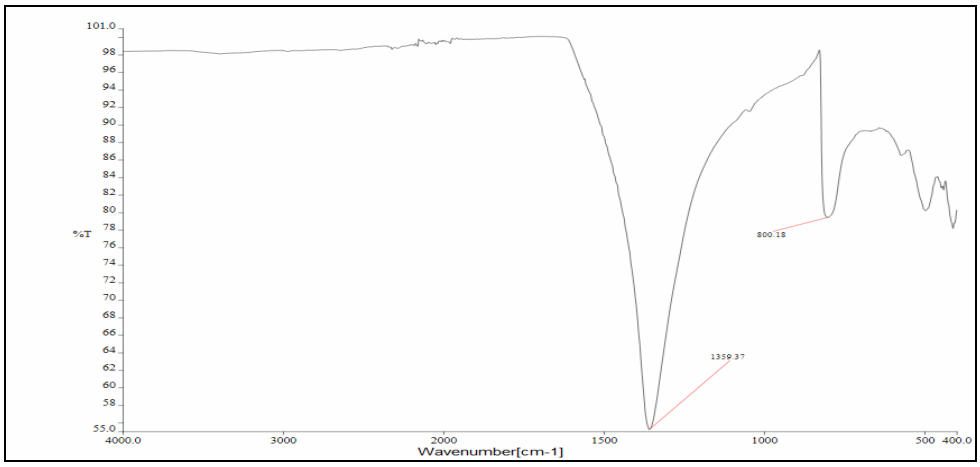

Figure A.1.12. FTIR spectrum of hBN in presence of ZrO_2 1450°C.

Appendix A. 2. FTIR Spectra of hBN Samples at 1300°C

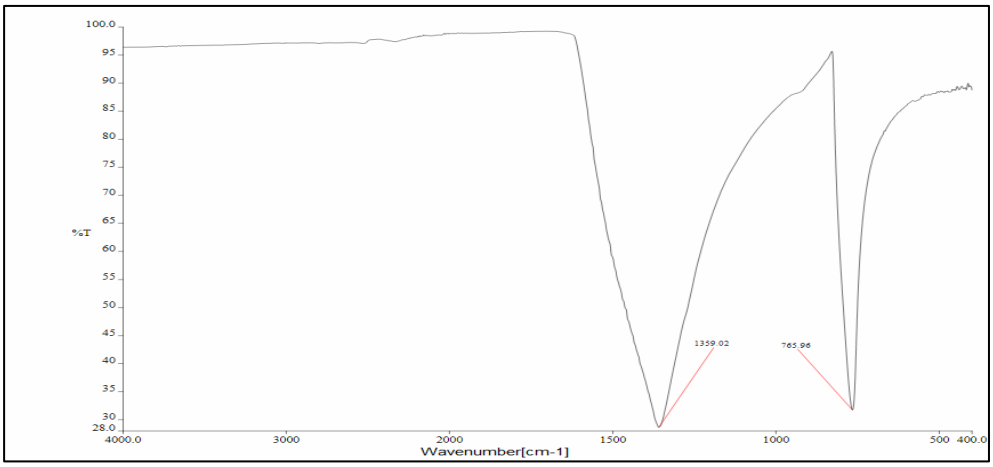

Figure A.2.1. FTIR spectrum of hBN in presence of BaO 1300°C.

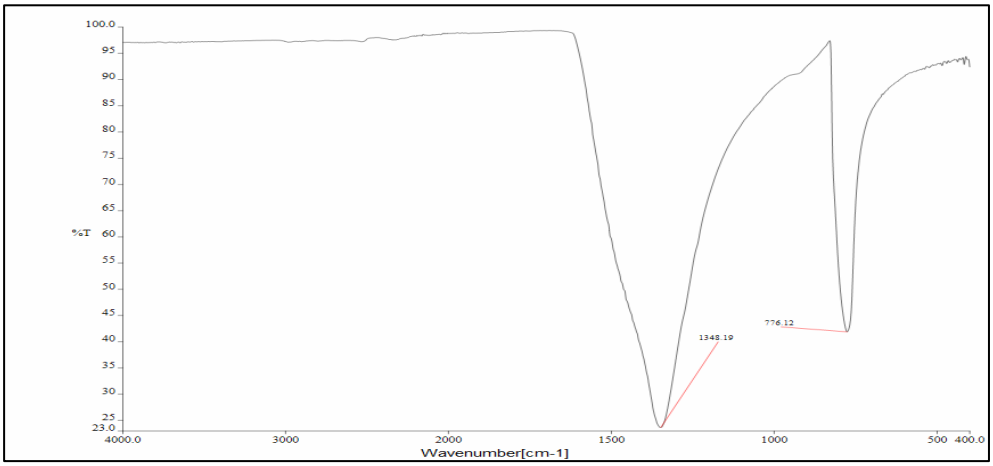

Figure A.2.2. FTIR spectrum of hBN in presence of CaO 1300°C.

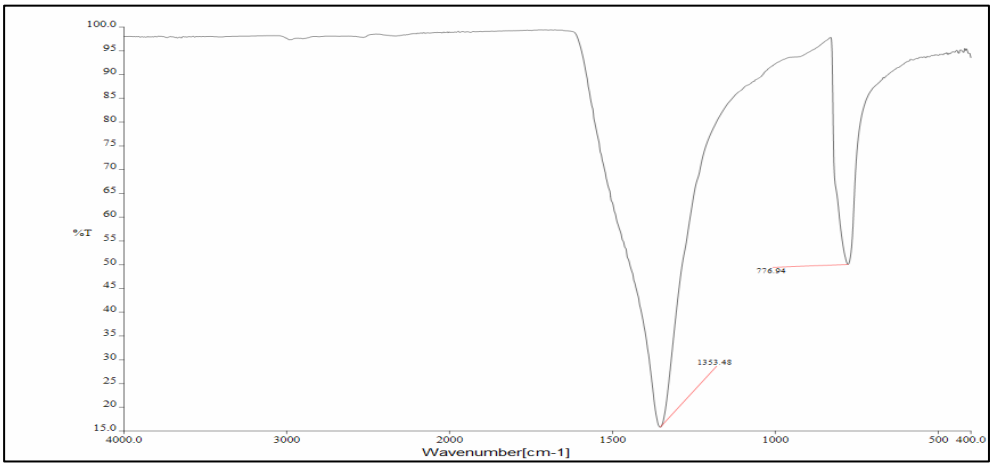

Figure A.2.3. FTIR spectrum of hBN in presence of La_2O_3 1300°C.

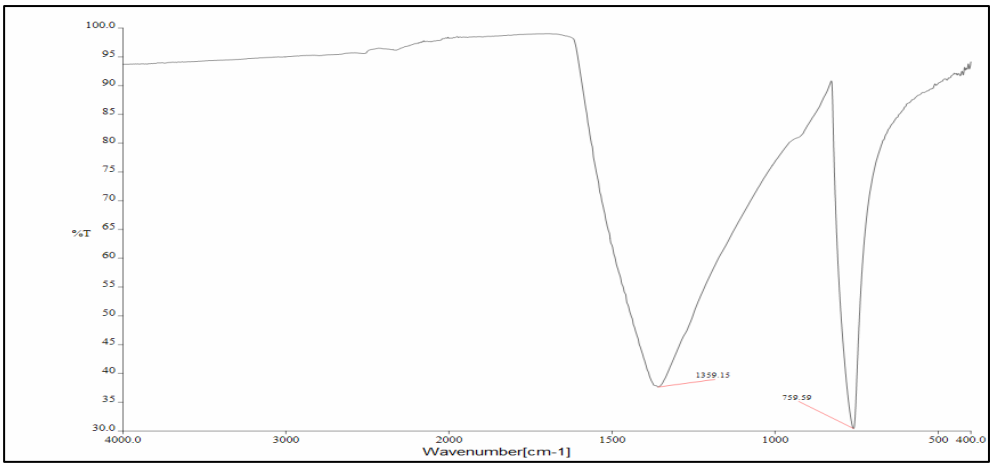

Figure A.2.4. FTIR spectrum of hBN in presence of Li_2O 1300°C.

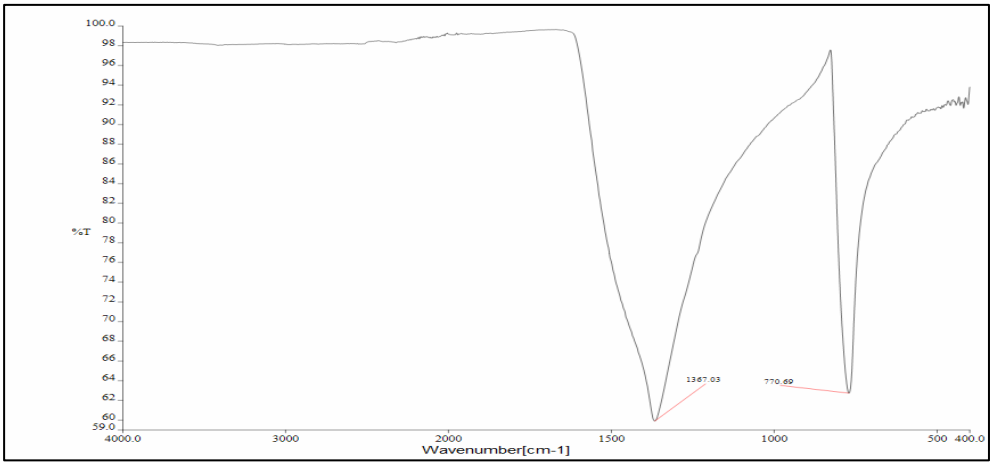

Figure A.2.5. FTIR spectrum of hBN in presence of MgO 1300°C.

Appendix A. 3. FTIR Spectra of hBN Samples at 1150°C

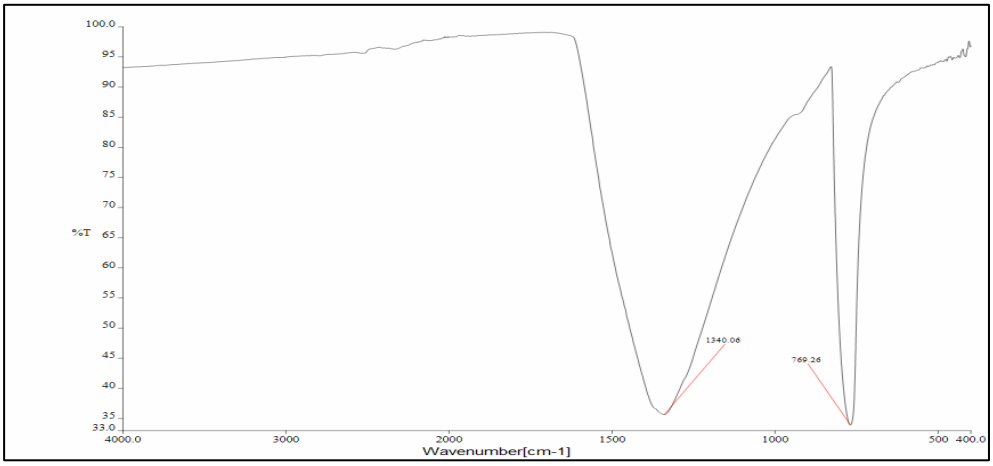

Figure A.3.1. FTIR spectrum of hBN in presence of Li_2O 1150°C.

Appendix A. 4. FTIR Spectra of hBN Samples at 1000°C

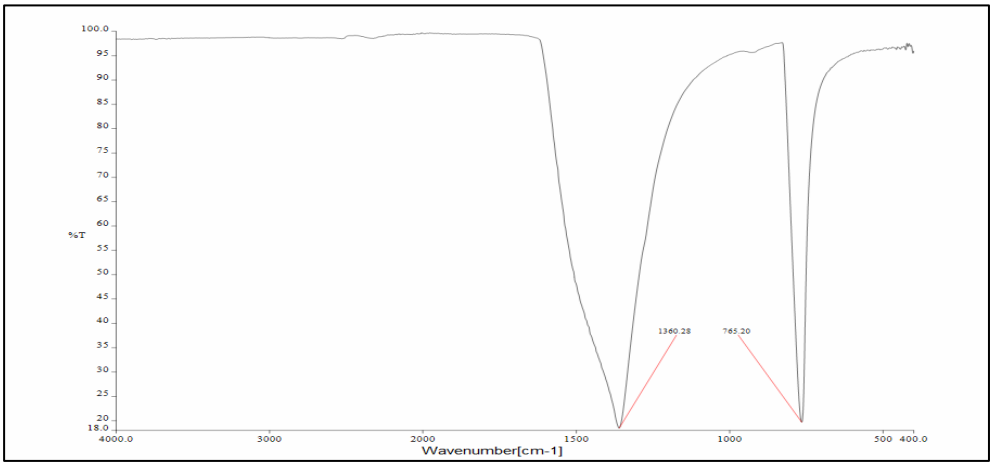

Figure A.4.1. FTIR spectrum of hBN in presence of Li_2O 1000°C.

Appendix B. XRD pattern of hBN Samples

Appendix B.1. XRD pattern of hBN Samples at 1450°C

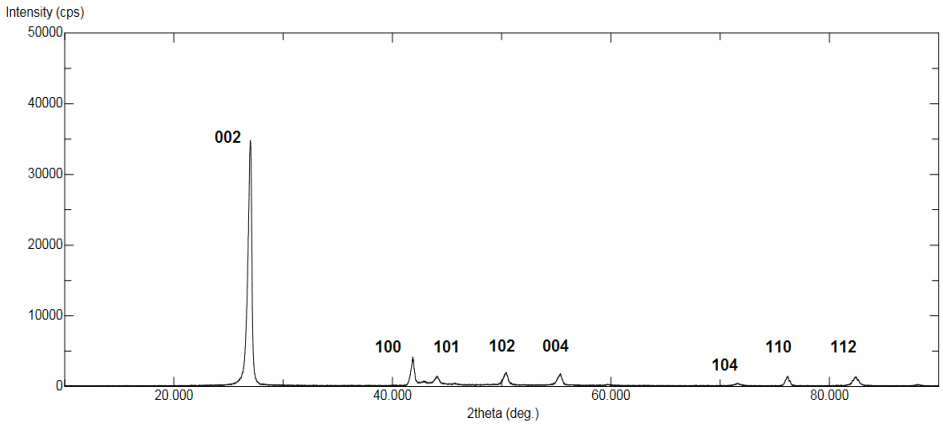

Figure B.1.1. XRD pattern of hBN in presence of BaO 1450°C.

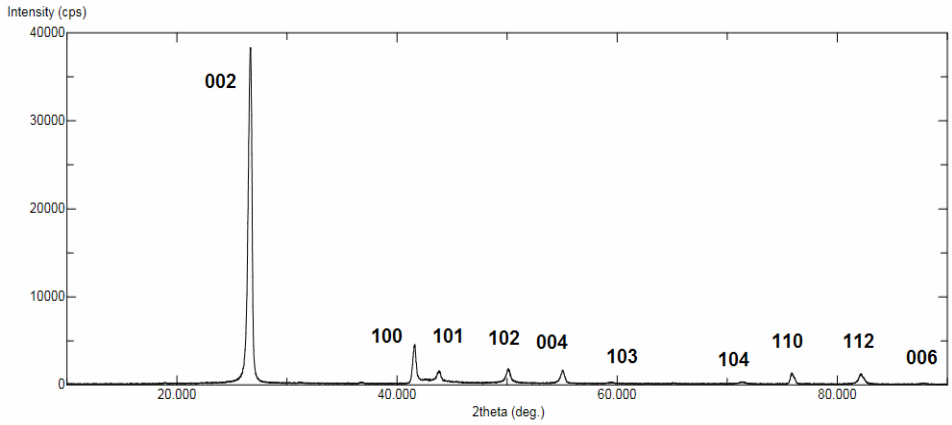

Figure B.1.2. XRD pattern of hBN in presence of CaO 1450°C.

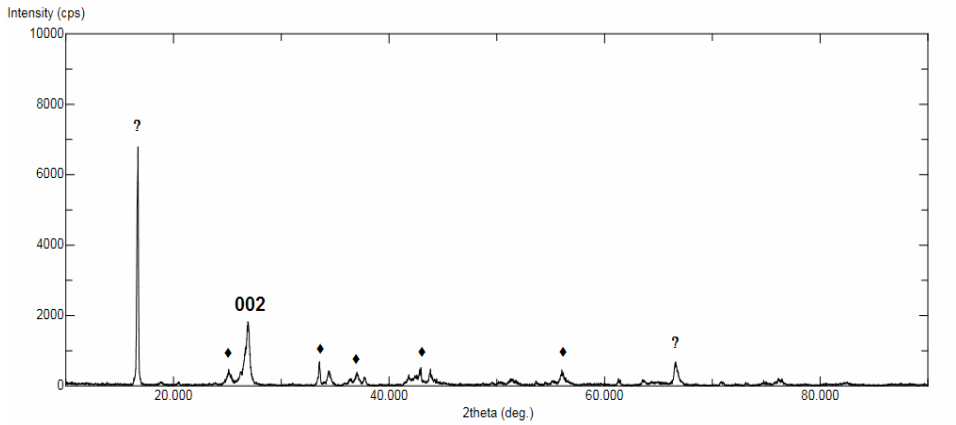

Figure B.1.3. XRD pattern of hBN in presence of Cr_2O_3 1450°C (♦: Cr_2O_3 peaks).

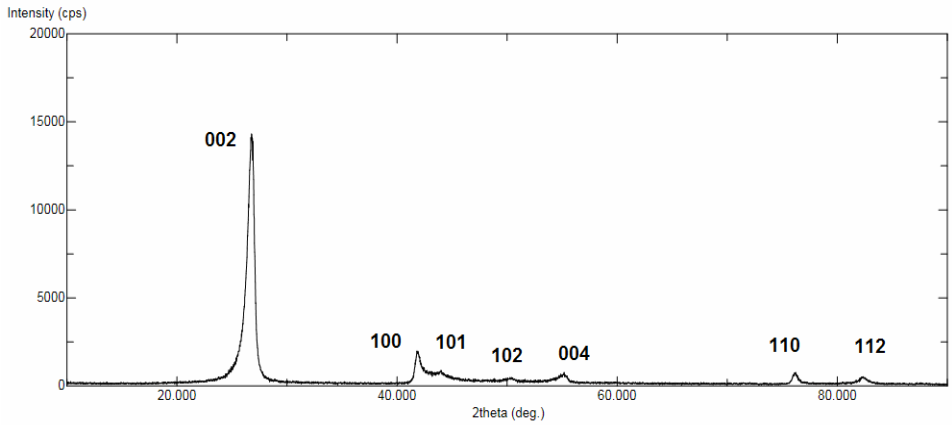

Figure B.1.4. XRD pattern of hBN in presence of La_2O_3 1450°C.

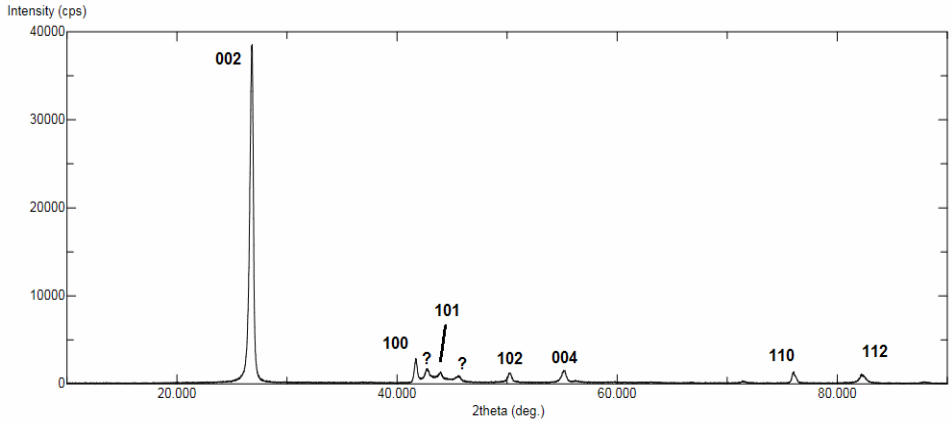

Figure B.1.5. XRD pattern of hBN in presence of Li_2O 1450°C.

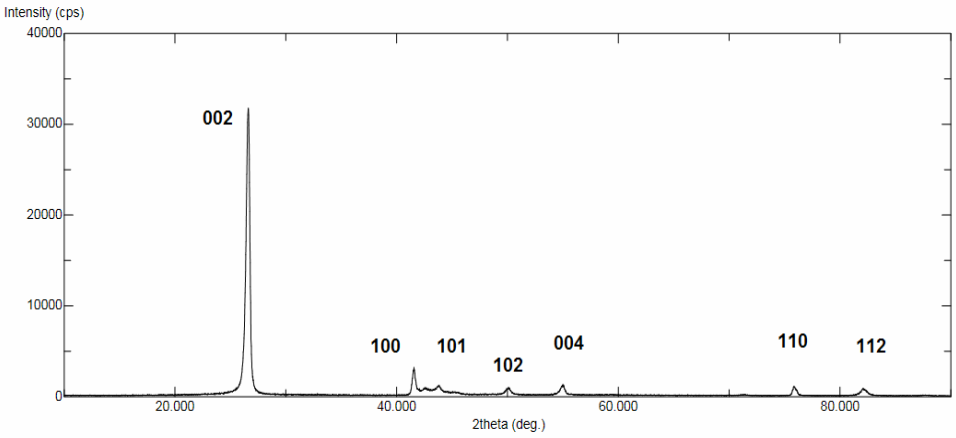

Figure B.1.6. XRD pattern of hBN in presence of MgO 1450°C.

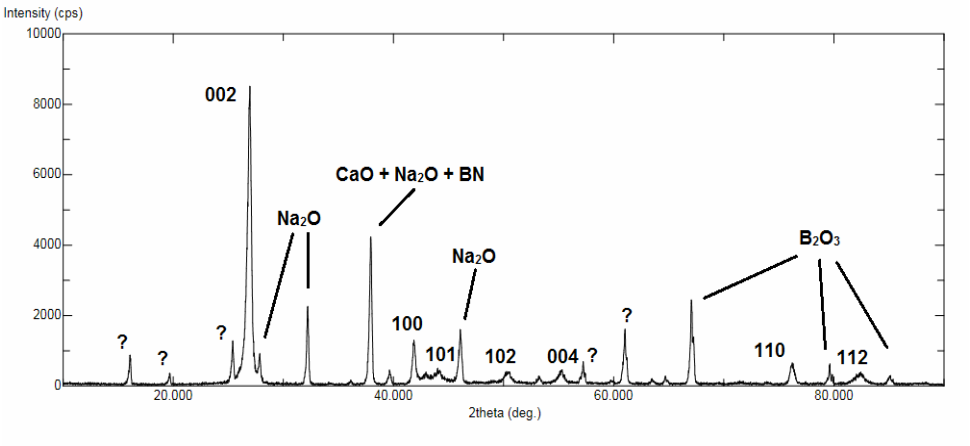

Figure B.1.7. XRD pattern of hBN in presence of Na_2O 1450°C.

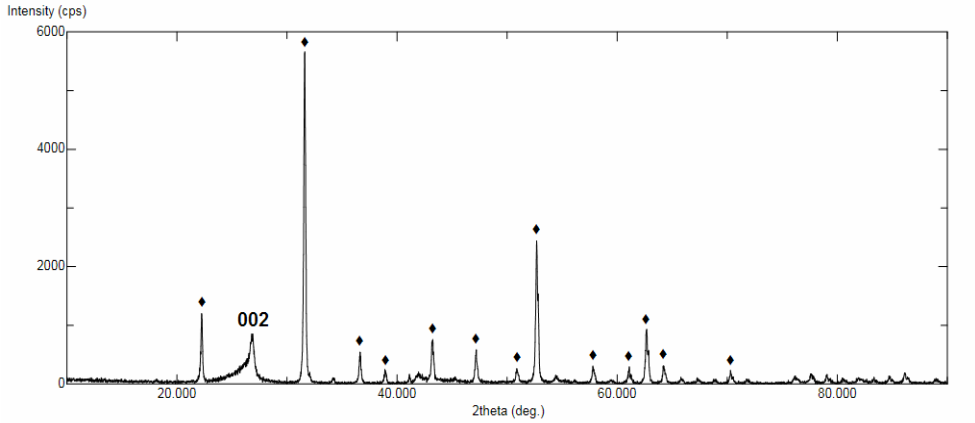

Figure B.1.8. XRD pattern of hBN in presence of Sc_2O_3 1450°C (♦: Sc_2O_3 peaks).

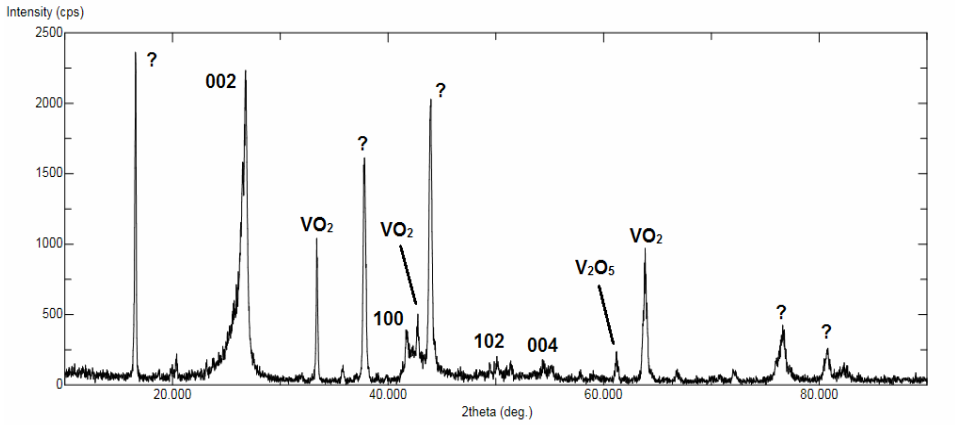

Figure B.1.9. XRD pattern of hBN in presence of V_2O_5 1450°C.

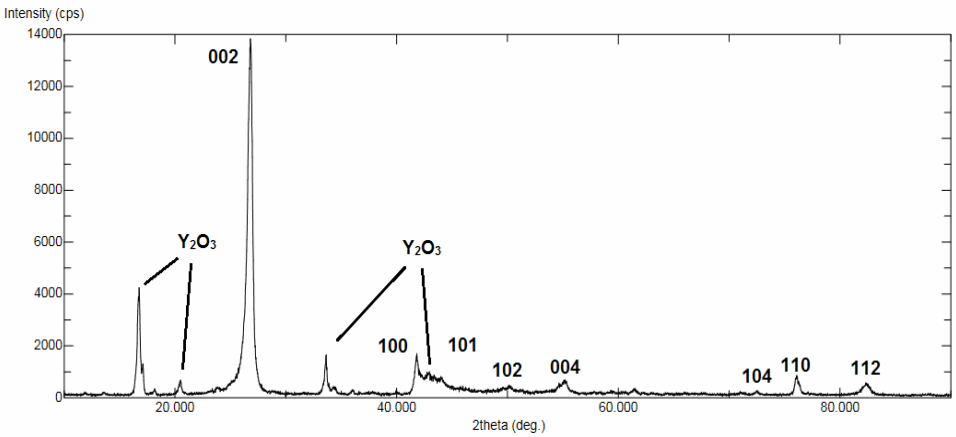

Figure B.1.10. XRD pattern of hBN in presence of Y_2O_3 1450°C.

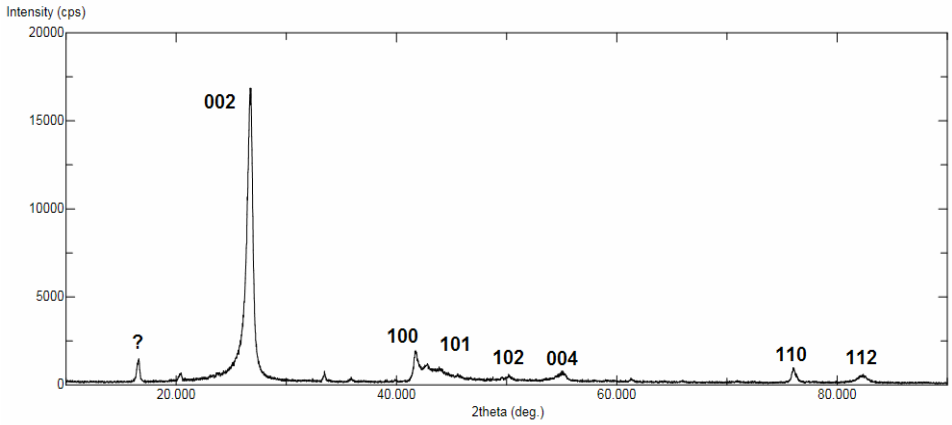

Figure B.1.11. XRD pattern of hBN in presence of ZnO 1450°C.

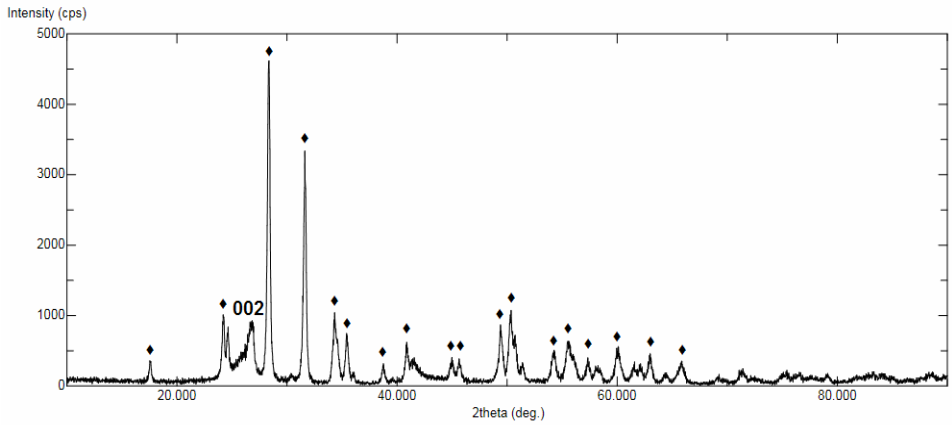

Figure B.1.12. XRD pattern of hBN in presence of ZrO_2 1450°C (♦: ZrO_2 peaks).

Appendix B.2. XRD pattern of hBN Samples at 1300°C

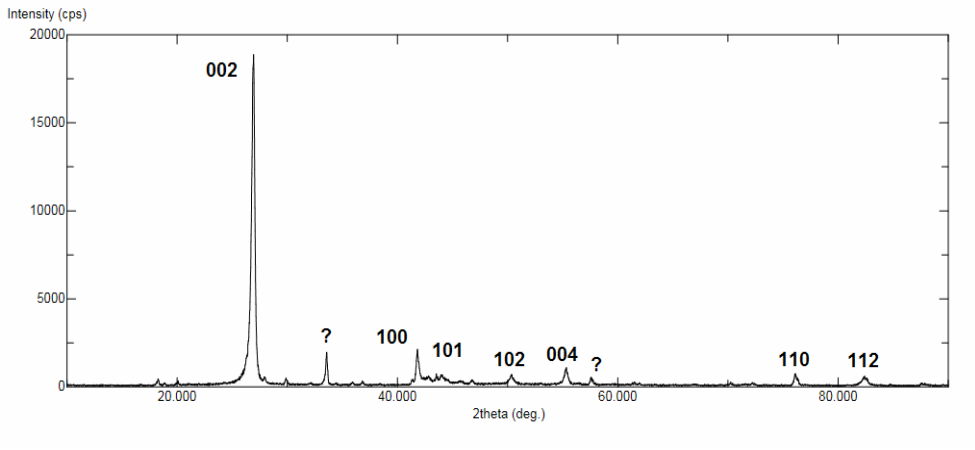

Figure B.2.1. XRD pattern of hBN in presence of BaO 1300°C.

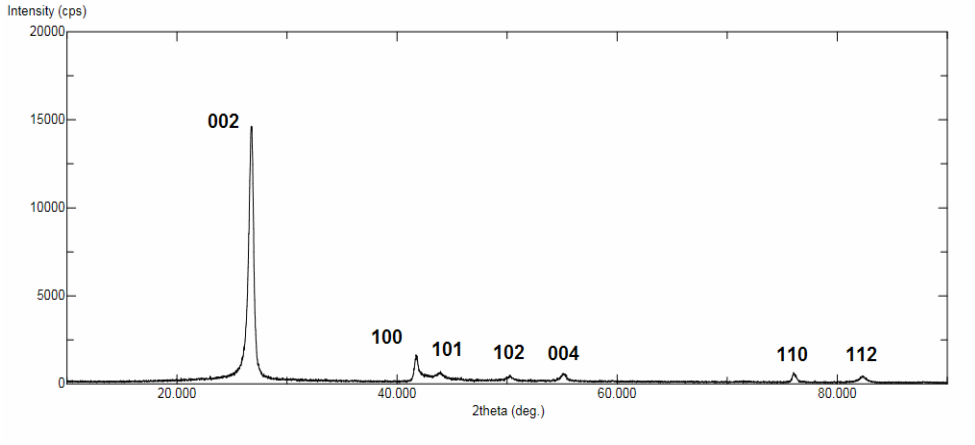

Figure B.2.2. XRD pattern of hBN in presence of CaO 1300°C.

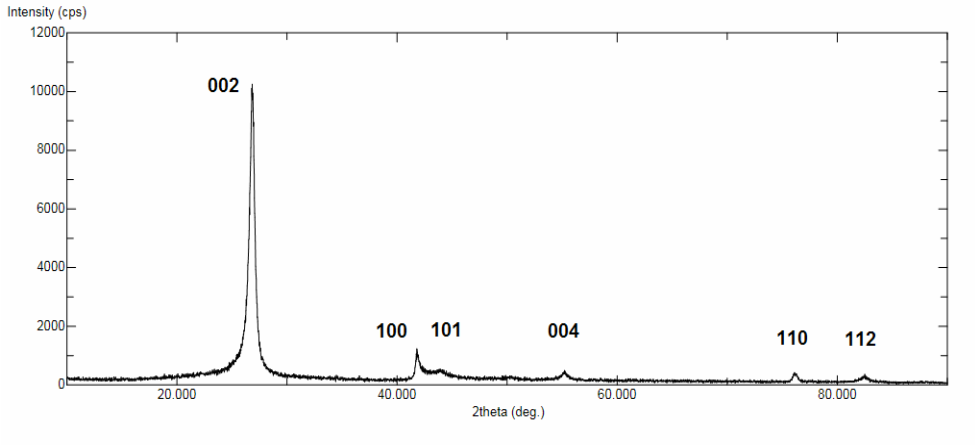

Figure B.2.3. XRD pattern of hBN in presence of La_2O_3 1300°C.

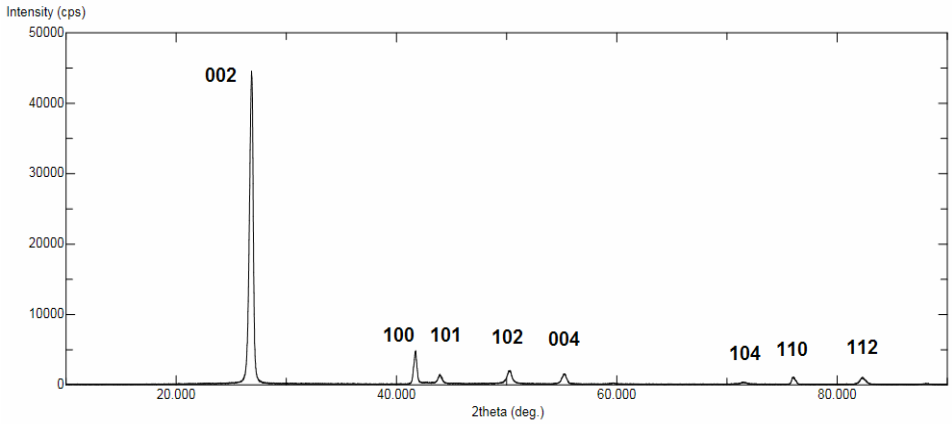

Figure B.2.4. XRD pattern of hBN in presence of Li_2O 1300°C.

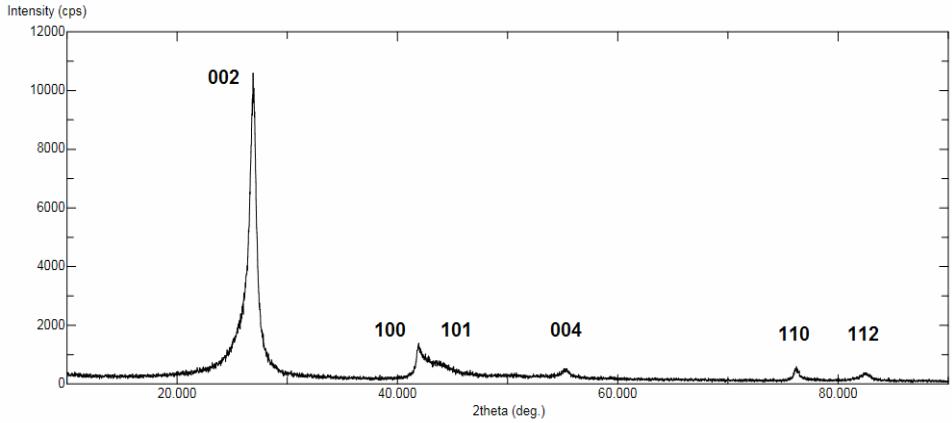

Figure B.2.5. XRD pattern of hBN in presence of MgO 1300°C.

Appendix B.3. XRD pattern of hBN Samples at 1150°C

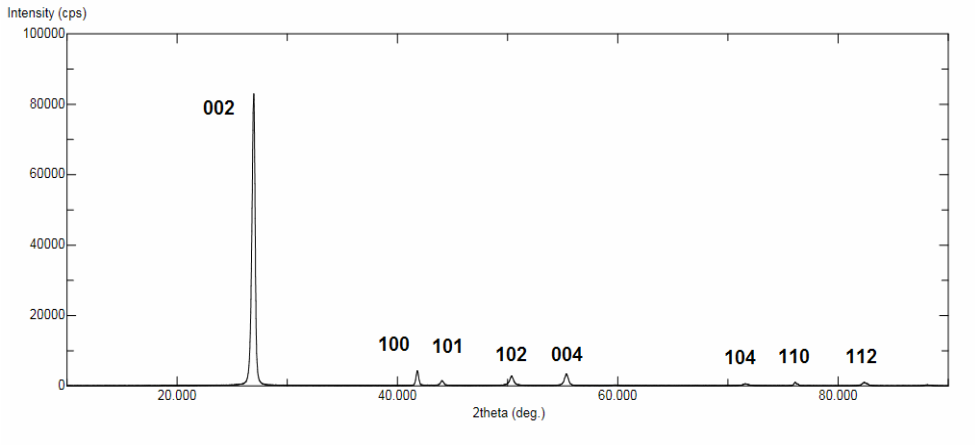

Figure B.3.1. XRD pattern of hBN in presence of Li_2O 1150°C.

Appendix B.4. XRD pattern of hBN Samples at 1000°C

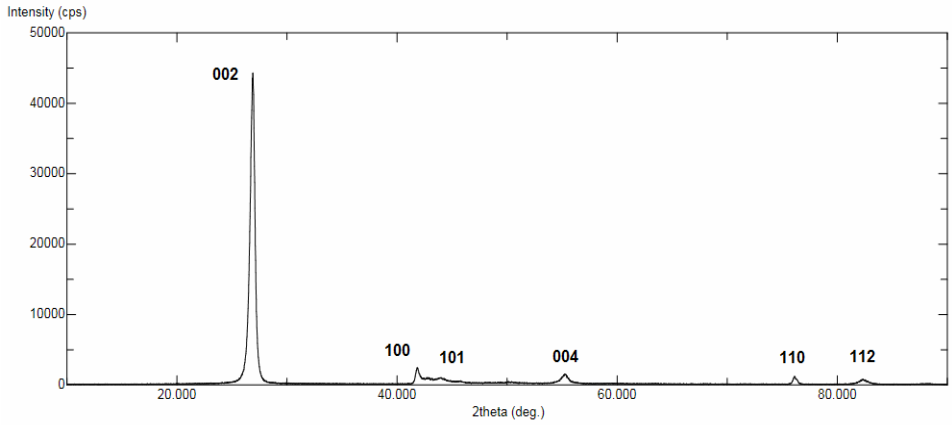

Figure B.4.1. XRD pattern of hBN in presence of Li_2O 1000°C.

Appendix C. SEM images of hBN Samples

Appendix C.1. SEM images of hBN Samples at 1450°C

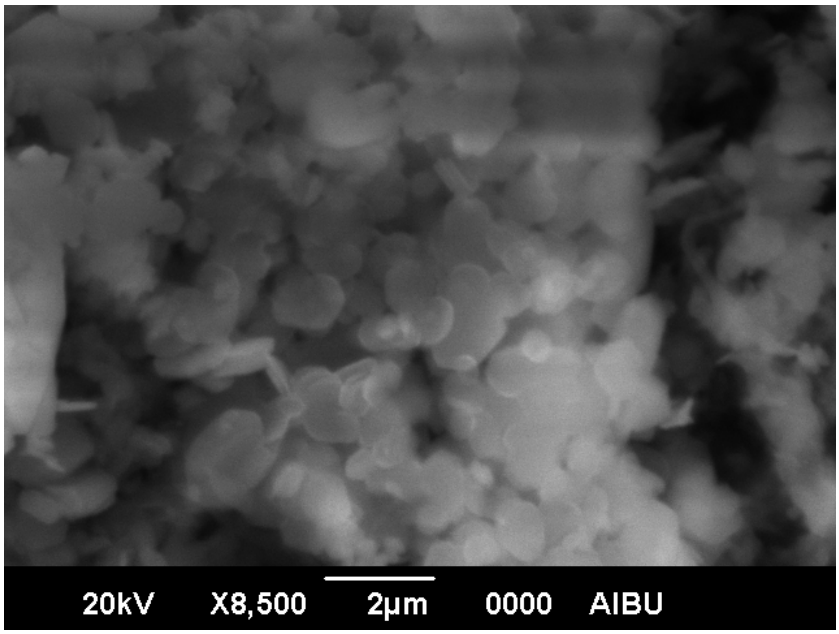

Figure C.1.1. SEM image of hBN in presence of BaO at 1450°C

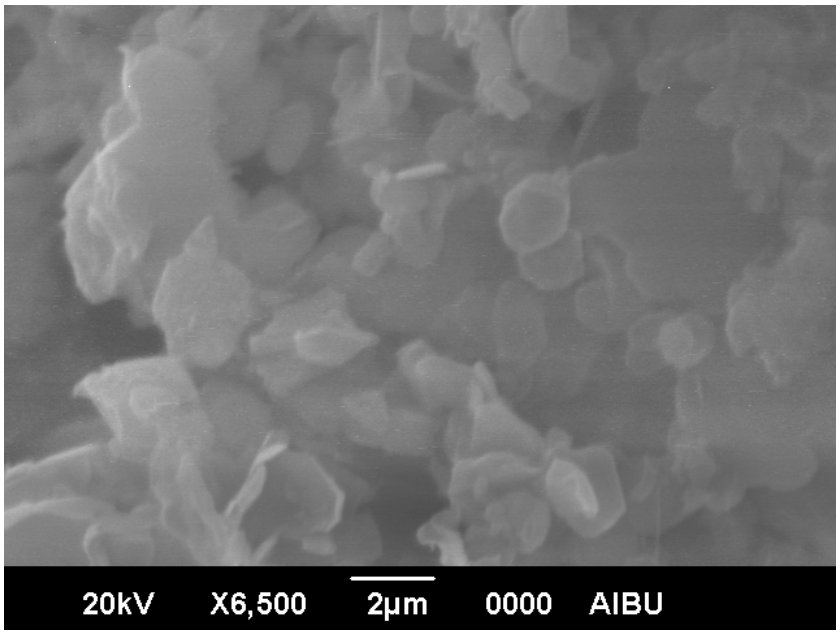

Figure C.1.2. SEM image of hBN in presence of CaO at 1450°C

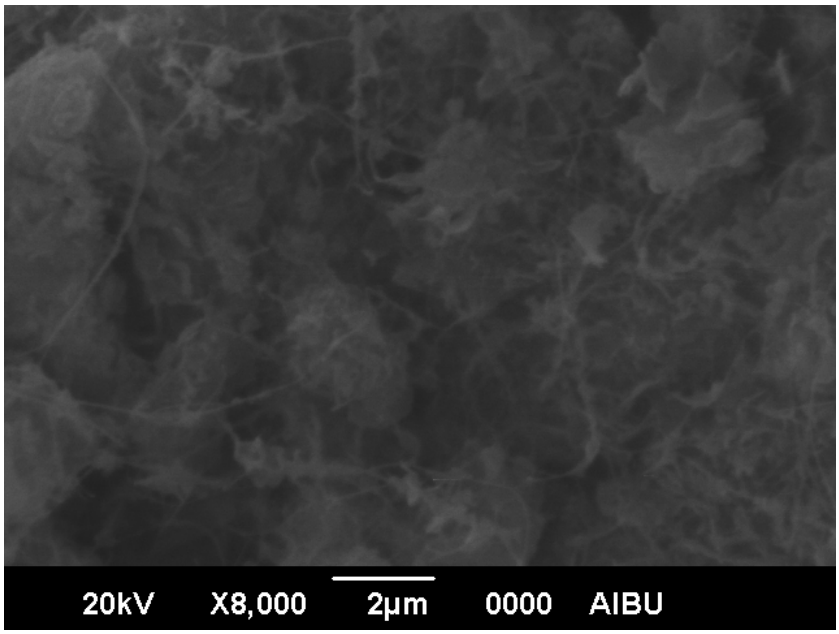

Figure C.1.3. SEM image of hBN in presence of La_2O_3 at 1450°C

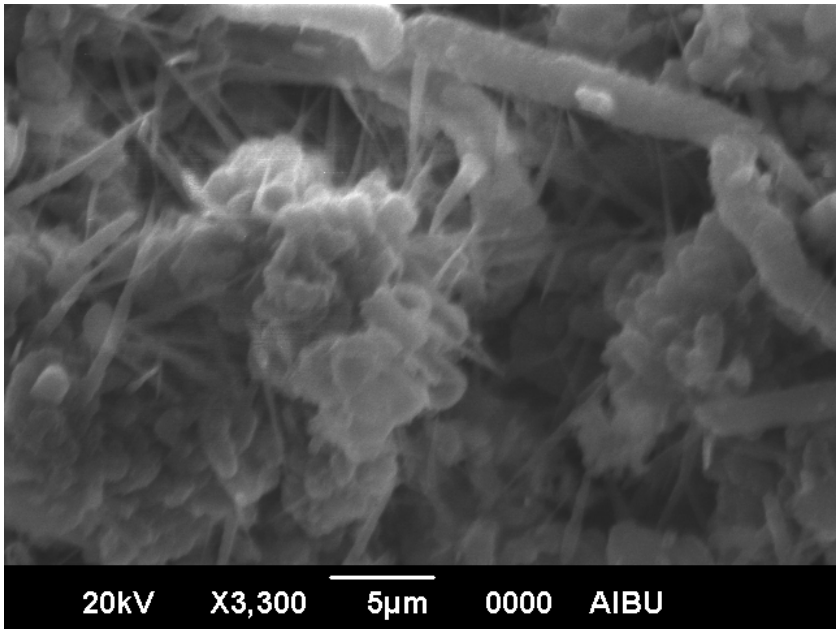

Figure C.1.4. SEM image of hBN in presence of Li_2O at 1450°C

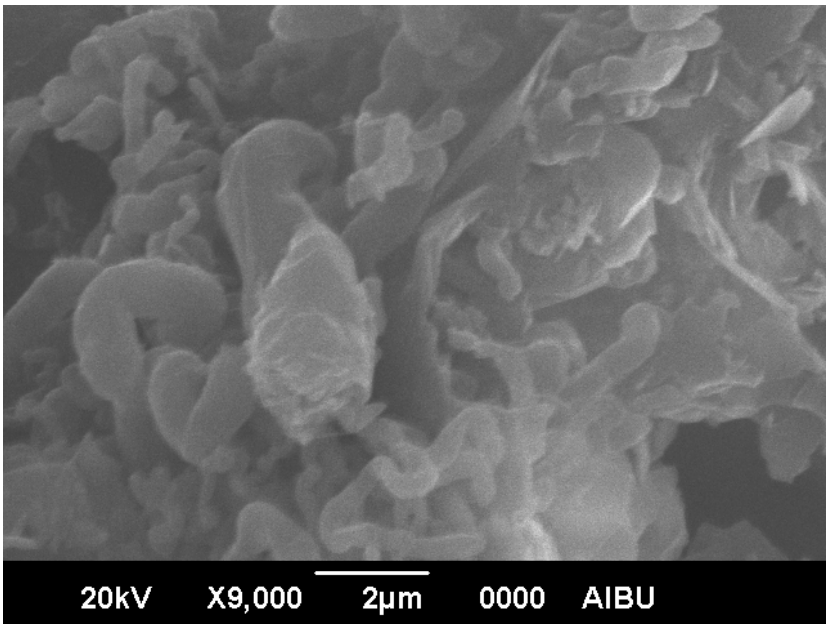

Figure C.1.5. SEM image of hBN in presence of MgO at 1450°C

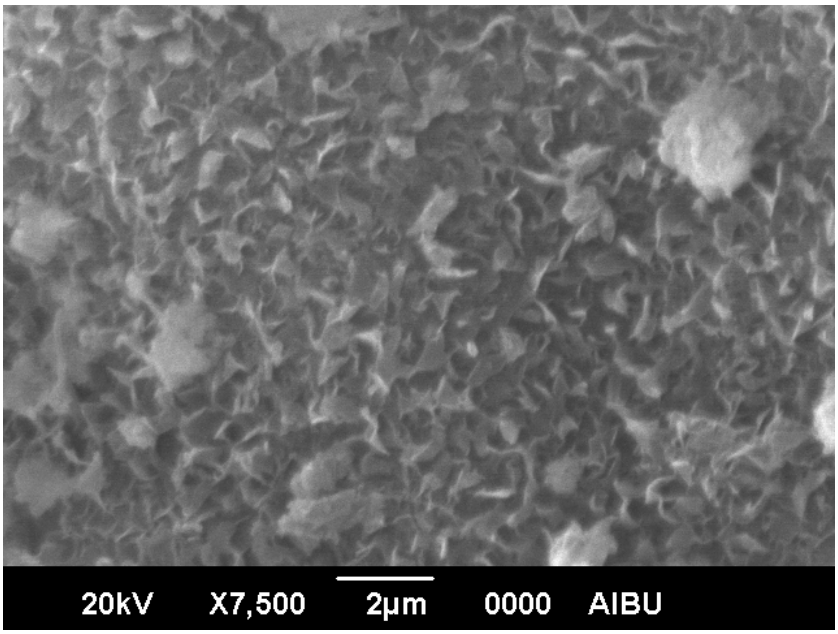

Figure C.1.6. SEM image of hBN in presence of ZnO at 1450°C

Appendix C.2. SEM images of hBN Samples at 1300°C

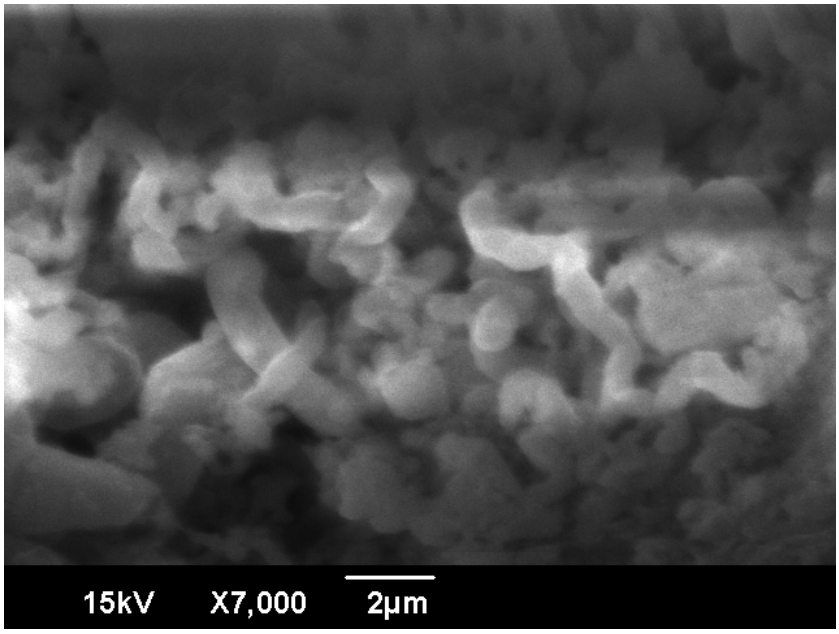

Figure C.2.1. SEM image of hBN in presence of BaO at 1300°C

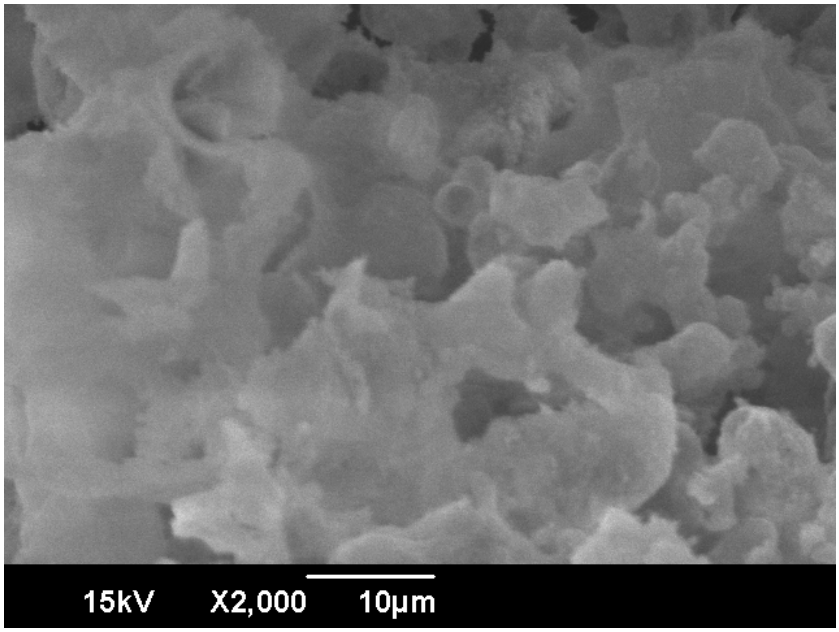

Figure C.2.2. SEM image of hBN in presence of CaO at 1300°C

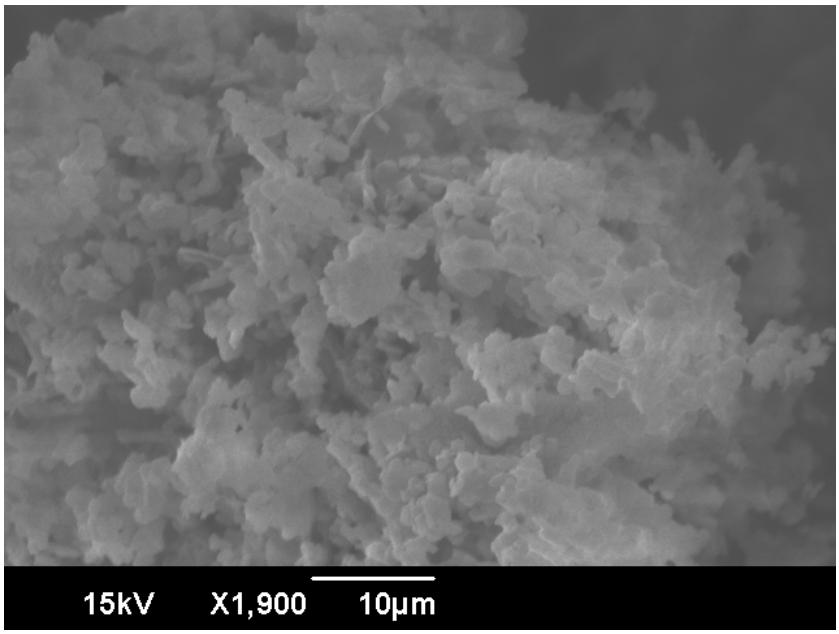

Figure C.2.3. SEM image of hBN in presence of Li_2O at 1300°C

Appendix C.3. SEM images of hBN Samples at 1150°C

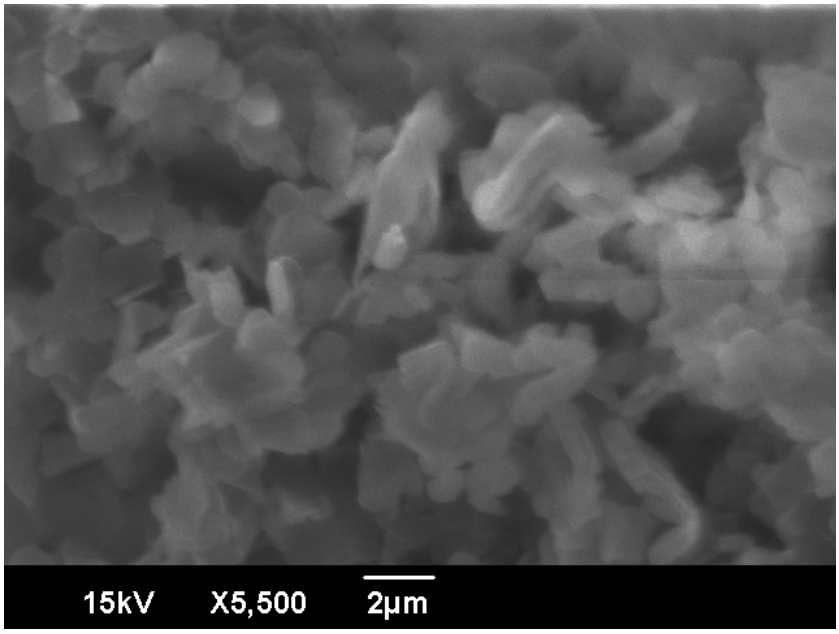

Figure C.3.1. SEM image of hBN in presence of Li_2O at 1150°C

Appendix C.4. SEM images of hBN Samples at 1000°C

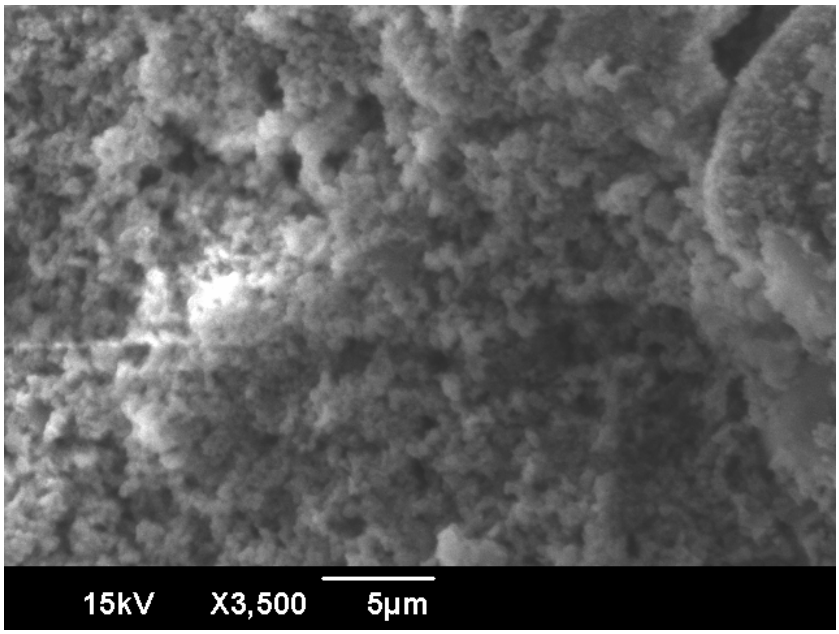

Figure C.4.1. SEM image of hBN in presence of Li_2O at 1000°C

8. CURRICULUM VITAE

Name SURNAME	**:**	**Erkam GÜLLÜOĞLU**
Place and Date of Birth	**:**	**Çatalca 12.12.1985**
Universities		
Bachelor's Degree	**:**	**Abant Izzet Baysal University**
e-mail	**:**	**erkamgulluoglu@gmail.com**
Address	**:**	
List of Publications	**:**	
Awards	**:**	
Hobbies (Optional)	**:**	